ENGINEERING RESEARCH INSTITUTE
THE UNIVERSITY OF MICHIGAN
ANN ARBOR

Final Report

AN EXPERIMENTAL INVESTIGATION OF THE STABILITY OF AXIALLY SYMMETRIC POISEUILLE FLOW

Reports Control No. OSR-TR-56-2

Richard J. Leite

Arnold M. Kuethe
Project Supervisor

Project 2072

DEPARTMENT OF THE AIR FORCE
AIR RESEARCH AND DEVELOPMENT COMMAND
CONTRACT NO. AF 18(600)-350

November 1955

This report has also been submitted as a dissertation in partial fulfillment of the requirements for the degree of Doctor of Philosophy in The University of Michigan, 1956.

TABLE OF CONTENTS

LIST OF ILLUSTRATIONS

LIST OF ILLUSTRATIONS (continued)

LIST OF ILLUSTRATIONS (concluded)

ACKNOWLEDGMENT

The author is happy to express his deep appreciation to Professors Arnold M. Kuethe and John R. Sellars. The program was under the supervision of Professor Kuethe who, along with Professor Sellars, was always available for advice and guidance during the course of the experiments and for consultation concerning interpretation of the results. The theoretical work of Professor Sellars and Dr. Gilles M. Corcos was an invaluable guide during the course of the experiments.

Special appreciation is extended to Professor Robert C. F. Bartels, Dr. Mahinder S. Uberoi and Messrs. Louis C. Garby, Leonard J. Pernick, K. R. Raman and Robert L. Roensch for their helpful suggestions and assistance.

ABSTRACT

The purpose of this experimental study was to investigate the stability of Poiseuille flow and compare the experimental results with the theoretical predictions of a recent unpublished mathematical analysis of the problem by Corcos and Sellars. A review of this theory is presented and experimental results are compared with its predictions.

A detailed description of the method used to obtain axially symmetric undisturbed laminar flow of air in a pipe is given. Temperature gradients in the settling chamber, located upstream of the pipe, caused the maximum velocity point of the parabolic velocity distribution to lie below the centerline of the pipe. An asymmetric addition of heat in the settling chamber provided a means of correcting for the adverse temperature gradients. No tendency of the undisturbed flow to become turbulent was detected up to a maximum Reynolds number of approximately 20,000, the maximum capacity of the air supply system. Tests were not made at this Reynolds number because of unsteadiness in the laboratory air supply.

Hot-wire anemometer measurements were made in fully developed laminar flow in a smooth lucite pipe having an internal diameter of 1.25 inches and a length of 73 feet at Reynolds numbers of 4,000, 6,600 and 13,000. Small, nearly axially symmetric disturbances were superimposed upon the mean flow by longitudinal oscillations of a sleeve immediately adjacent to the inner wall of the pipe. The frequency and amplitude of this motion could be continuously controlled over a suitable range of values. Radial traverses of the disturbed flow field gave amplitude and relative phase angle variations across the pipe while longitudinal surveys provided means of computing wave velocities and damping factors of the disturbances. Results of several typical radial, peripheral and longitudinal surveys are presented. These surveys indicate that the disturbance does not achieve complete equilibrium before it is completely damped. Nonaxial symmetry of the disturbances in interpreted as a superposition of axially and nonaxially symmetric components. Measurements indicate that the nonaxially symmetric components decay at least as rapidly as axially symmetric disturbances.

Some brief observations of the effects of large disturbances are presented also. The fact that the onset of turbulent flow is not an instantaneous phenomenon appears to be a rather significant result of these observations. Large disturbances appear to undergo a systematic distortion as an intermediate step in the establishment of the fully turbulent state. When a turbulent wake was introduced at a mid-radial position, initially the wake diffused radially with little effect on the velocity profile. At a distance of 47 diameters downstream both the turbulence distribution

and the velocity profile were near those for fully developed turbulent flow.

The results are presented in the form of curves showing undisturbed velocity profiles, with and without heat addition; radial, peripheral and longitudinal disturbance distributions; comparison of experimental results with small perturbation theory; transition to turbulent flow through a systematic distortion of large disturbances; and the radial diffusion of a turbulent wake until turbulent flow completely fills the pipe.

Several general conclusions can be drawn from this experimental investigation: (1) Poiseuille flow is stable when perturbed by small axially symmetric or nonaxially symmetric disturbances within the Reynolds number range investigated, (2) the rate of decay and speed of propagation of disturbances are in satisfactory agreement with theory, and (3) the onset of turbulent flow in fully developed laminar pipe flow, when large disturbances are imposed, is not an instantaneous phenomenon but one that takes place through a relatively regular process of growth and diffusion of the disturbance.

OBJECTIVE

The purpose of this experimental study was to investigate the stability of Poiseuille flow and compare the experimental results with theoretical predictions.

Unclassified

BIBLIOGRAPHICAL CONTROL SHEET

1. Originating agency and/or monitoring agency:

   O.A.: The University of Michigan, Ann Arbor, Michigan
   M.A.: Headquarters, ARDC, Office of Scientific Research

2. Originating agency and/or monitoring agency report number:

   O.A.: UM-ERI Report
   M.A.: OSR Technical Report OSR-TR-56-2

3. Title and classification of title: AN EXPERIMENTAL INVESTIGATION OF THE STABILITY OF AXIALLY SYMMETRIC POISEUILLE FLOW (UNCLASSIFIED)

4. Personal authors: Leite, Richard J.

5. Date of report: November 1955

6. Pages: 82 + 10 preliminary

7. Illustrative material: 43 figures

8. Prepared for Contract No.: AF 18(600)-350

9. Prepared for Project Code(s) and/or No.(s): R-352-40-1

10. Security classification: UNCLASSIFIED

11. Distribution limitations: None

12. Abstract: This report contains the results of an experimental investigation of the stability of axially symmetric Poiseuille flow. A review of a recent mathematical formulation of the problem is presented. Experimental results are in satisfactory agreement with this theory, which predicts that the flow is stable to small axially symmetric disturbances. A description of the methods utilized to obtain axially symmetric laminar flow, superimpose small periodic disturbances and observe the distribution and propagation of the disturbances is given. A maximum Reynolds number of 13,000 was used. Brief observations of transition through a reproducible distortion of large disturbances and the diffusion of a turbulent wake indicate that the onset of the turbulent regime is not an instantaneous phenomenon.

INTRODUCTION

Since Osborne Reynolds first conducted his experiments in a circular pipe, many investigations, both theoretical and experimental, have revealed much information concerning many aspects of Poiseuille flow. Through these investigations, determinations of mean velocity distribution and its development to a steady state condition, friction factors for both laminar and turbulent flow, introduction of secondary flows at pipe bends, etc., have received extensive attention. For the most part, primary interest appeared to be concerned with the general overall effects resulting from various external factors, such as pipe length, wall smoothness, alignment and initial disturbances. These general overall effects included transition from laminar to turbulent flow in both the laminar transition and fully developed laminar flow states. Other investigators, such as Laufer,[19] have dealt with fully developed turbulent flow.

In early investigations the determination of so-called "critical Reynolds number" was the principle objective. Little emphasis appeared to be placed upon the laminar flow regime in which the tests were conducted and little effort was directed towards an identification of the source of the disturbances which ultimately lead to transition. The upper limit of the critical Reynolds number then attracted some interest. As Prandtl[20] points out, results seemed to indicate that there is no definite upper limit to the critical Reynolds number and that it can be made to exceed any value by reduction of initial disturbances. The critical region is in the inlet region of the pipe where the boundary layer is thin. Here free stream disturbances can contaminate the boundary layer, which has definite stability criteria, and cause the entire flow field to become

turbulent as a result of the presence of large initial disturbances or or the amplification of particular small disturbances.

A recent theoretical study by Tatsumi[21] indicates that there exists a definite minimum critical Reynolds number below which all small disturbances in the inlet flow will be damped. He has shown the existence of a neutral stability curve which depends upon the distance downstream of the inlet. However, since, as will be shown later, the fully developed flow is stable to small disturbances, disturbances originating in the inlet region will damp when they reach the region of fully developed flow, unless their amplitude is great enough to exceed the range of application of the stability theory.

Other experiments in the fully developed laminar flow region have had somewhat different objectives than the present work. Rothfus and Prengle[22] were concerned with transition due to initial disturbances but it is doubtful whether their results are significant due to disturbances introduced by the dye ejector and possible secondary flow disturbances in the inlet region. Weske and Plantholt[23] were interested in the behavior of discrete vortex systems which were introduced asymmetrically into fully developed pipe flow. While there appear to be indications in previous work that fully developed pipe flow is stable, the investigation reported here is the first quantitative experimental study of the stability of fully developed laminar flow to small disturbances. Several theoretical investigations have been attempted but only very recently did Corcos and Sellars[14] complete what is believed to be the entire mathematical formulation of the stability problem.

The preliminary work of the above authors provided the initial stimulation to attempt an experimental investigation of the stability problem.

At that time it was not known whether the mathematical picture was correct or not, in fact, there was some doubt because computer results (reference 11) did not agree with the results of Pekeris.[10] Then it was found that Pekeris had solved only a portion of the problem, and that the unsolved portion provided predictions for the practical case. The theoretical problem was completed almost simultaneously with the completion of the experiments and the results of the two are in satisfactory agreement. Therefore, it appears that within the range of Reynolds numbers covered in this experiment the flow is stable to small disturbances and the theory does describe the physical phenomenon.

What follows is a description of the experimental apparatus and techniques used in conducting the necessary tests. An attempt to include all the essential details was made so that a continuation of the present work can be made without excessive duplication of effort especially in the establishment of axially symmetric flow.

It is hoped that this work will stimulate others to renew their interest in this problem and as a result lead to a complete analysis of the problem of stability of fully developed laminar flow in a pipe.

REVIEW OF THEORETICAL INVESTIGATIONS

By the end of the last century interest in stability of fluid motions had grown considerably. However, it was not until 1906-8 when Orr[1] and Sommerfeld[2] first formulated the disturbance equations from the equation of motion and equation of continuity for the cases of two-dimensional and axially symmetric flows, that much impetus was given to the problem. These authors were unable to accomplish much beyond the derivation of the problem because of the complex type of periodic disturbance they assumed. Due to the extremely difficult mathematics involved, little work was done to obtain solutions until a contribution by Heisenburg[3] initiated renewed interest in the problem as a whole. Heisenburg's methods were improved by Tollmien[4] and Schlichting,[5] both of whom studied the two-dimensional Blasius and Couette flows and predicted that instability could be induced by the amplification of infinitesimal disturbances originating within the boundary layer. This result was viewed with suspicion by workers in the field because disturbances of this nature had not been observed during experimental investigations. In addition, the mathematical difficulties were so extensive, both theoretically and practically, that combined with the above physical uncertainty, the net result was a lack of interest in the problem.

The experimental work of Schubauer and Skramstad[6] initiated renewed interest by showing that disturbances of the type predicted by Tollmien[4] and Schlichting[5] actually existed within the boundary layer and that they introduced an instability which could result in transition. Following this discovery, C. C. Lin[7] working on the theoretical approach to the problem resolved most of the mathematical difficulties.

Prior to the above experimental work, there were essentially two schools of thought concerning the cause of transition. G. I. Taylor[8] and others took the view that finite disturbances from the main stream entering the boundary layer developed adverse pressure gradients and eventually caused separation to occur. The other viewpoint was that certain infinitesimal disturbances within the boundary layer, aided by proper conditions, grew with respect to time and eventually achieved large enough magnitudes to cause transition to turbulent flow. Schubauer and Skramstad[6] substantiated the second viewpoint. Therefore, since the first mechanism was already accepted as a possible cause of transition, this work indicated that both viewpoints were legitimate.

The above discussion has been a general resume of the advances made in the field of stability of laminar flow. In the present work however, we are concerned with the stability of fully developed axially symmetric laminar flows, and therefore we will proceed to the theoretical work in that field by first indicating how the disturbance equation is developed from the equations of motion and continuity.

For an incompressible viscous fluid having axial symmetry two equations of motion exist, namely:

$$\frac{\partial \bar{u}}{\partial t} + \bar{u}\frac{\partial \bar{u}}{\partial x} + \bar{w}\frac{\partial \bar{u}}{\partial r} = -\frac{1}{\rho}\frac{\partial \bar{p}}{\partial x} + \nu\left[\frac{\partial^2 \bar{u}}{\partial x^2} + \frac{1}{r}\frac{\partial \bar{u}}{\partial r} + \frac{\partial^2 \bar{u}}{\partial r^2}\right], \quad (2.1)$$

$$\frac{\partial \bar{w}}{\partial t} + \bar{u}\frac{\partial \bar{w}}{\partial x} + \bar{w}\frac{\partial \bar{w}}{\partial r} = -\frac{1}{\rho}\frac{\partial \bar{p}}{\partial r} + \nu\left[\frac{\partial^2 \bar{w}}{\partial x^2} - \frac{\bar{w}}{r^2} + \frac{1}{r}\frac{\partial \bar{w}}{\partial r} + \frac{\partial^2 \bar{w}}{\partial r^2}\right]. \quad (2.2)$$

and the equation of continuity becomes

$$\frac{\partial \bar{u}}{\partial x} + \frac{\bar{w}}{r} + \frac{\partial \bar{w}}{\partial r} = 0 \quad . \quad (2.3)$$

The x-axis coincides with the axis of the pipe and the r-axis is normal to it, Fig. 1. $\overline{u}$ and $\overline{w}$ are the total velocities in the x and r directions, respectively and ν is the kinematic viscosity.

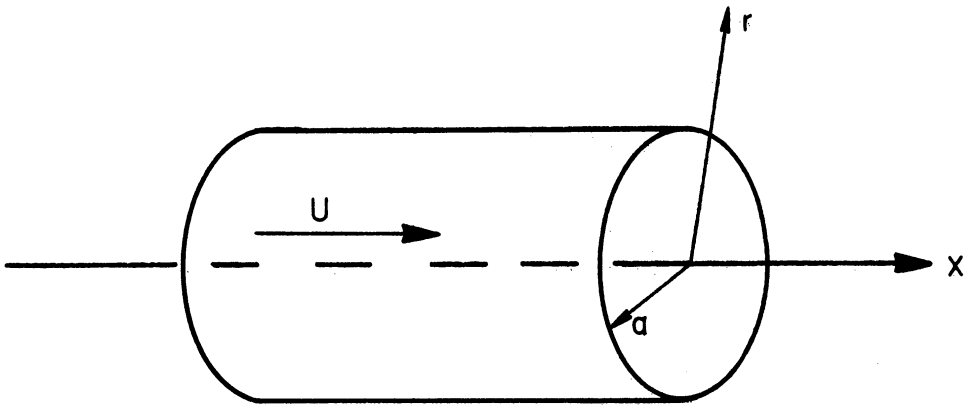

Fig. 1. Coordinate system.

We now assume that

$$\overline{u} = U - u; \quad \overline{w} = w; \quad \overline{p} = P + p \tag{2.4}$$

where U is the steady-state undisturbed velocity in the direction of the x-axis and a function of r alone, P is the pressure in the undisturbed flow; u and w, the disturbance velocities, are small in comparison with U and $p << P$. Since it is assumed that steady-state conditions exist, $\partial U/\partial t = 0$. Substituting (2.4) into (2.1) and (2.2) and neglecting products of small quantities only, the pressure terms can be eliminated by cross differentiation. From (2.3) a stream function can be defined for the superimposed disturbance flow in the following manner:

$$u = -\frac{1}{r}\frac{\partial \psi}{\partial r}; \quad w = \frac{1}{r}\frac{\partial \psi}{\partial x} \quad . \tag{2.5}$$

This permits the disturbance equation to be written in terms of the axially symmetric stream function. In nondimensional form it appears as follows:

$$\left[\frac{\partial}{\partial t} + U\frac{\partial}{\partial x}\right]\left[\frac{\partial^2\psi}{\partial r^2} - \frac{1}{r}\frac{\partial\psi}{\partial r} + \frac{\partial^2\psi}{\partial x^2}\right] + \left[\frac{U'}{r} - U''\right]\frac{\partial\psi}{\partial x}$$

$$= \frac{1}{R}\left[\frac{\partial^4\psi}{\partial r^4} - \frac{2}{r}\frac{\partial^3\psi}{\partial r^3} + \frac{3}{r^2}\frac{\partial^2\psi}{\partial r^2} - \frac{3}{r^3}\frac{\partial\psi}{\partial r} + 2\frac{\partial^4\psi}{\partial r^2\partial x^2} + \frac{\partial^4\psi}{\partial x^4}\right] \qquad (2.6)$$

where primes denote differentiation with respect to r. $R = U_m a/\nu$ is defined where "a" is the radius of the pipe and U_m is the maximum undisturbed velocity in the flow field. The U that appears is nondimensional and varies from 0 to 1.

On the walls of the pipe both disturbance velocities must be zero while at the center $w = 0$ and u must remain finite. The boundary conditions in terms of ψ are

$$\frac{\partial\psi}{\partial r} = \frac{\partial\psi}{\partial x} = 0 \quad \text{at } r = 1, \quad \lim_{r\to 0}\left(\frac{1}{r}\frac{\partial\psi}{\partial x}\right) = 0$$
$$\lim_{r\to 0}\left(\frac{1}{r}\frac{\partial\psi}{\partial r}\right) \text{ is bounded} . \qquad (2.7)$$

Assuming that the functional dependence of ψ on r, x, and t can be separated in a simple way, it is then required that a solution of (2.6) be of the form

$$\psi(r,x,t) = \phi(r)\, e^{i\alpha(x-ct)} . \qquad (2.8)$$

Then an equation for the eigenfunctions, which is similar to the equation of Orr and Sommerfeld, can be written.

$$(U - c)(\phi'' - \phi'/r - \alpha^2\phi) + \phi(U'/r - U'')$$

$$= -\frac{i}{\alpha R}\left[\phi^{IV} - \frac{2}{r}\phi''' + \frac{3}{r^2}\phi'' - \frac{3}{r^3}\phi - 2\alpha^2\left(\phi'' - \frac{\phi'}{r}\right) + \alpha^4\phi\right] . \qquad (2.9)$$

The boundary conditions in terms of ϕ have the following form

$$\lim_{r \to 0} \left(\frac{\phi}{r}\right) \to 0, \quad \lim_{r \to 0} \left(\frac{\phi'}{r}\right) \text{ is bounded} \qquad (2.10)$$

$$\phi(1) = \phi'(1) = 0 .$$

The stability problem is now reduced to finding the behavior of the eigenvalues, c, as both α and R are allowed to vary. In general, c is complex so that $c = c_r + ic_i$, and the conditions that the disturbance amplifies, that it be neutral, and that it be damped, are simply $c_i > 0$, $c_i = 0$, and $c_i < 0$, respectively.

Several investigators have proceeded from this point towards a solution of the eigenvalue problem (2.9). The details of these investigations can be found in the references and therefore will not be given here. However, the essential features of each investigation will be presented.

The first study of the stability of Poiseuille flow to be reported was that of Sexl.[9] By expressing (2.9) as two simultaneous second order equations and using boundary conditions (2.10), he obtained solutions from which he concluded that the flow was stable, even though he gave no eigenvalues. His work has been criticized by Pekeris,[10] Sellars[11] and Corcos[12] on the grounds that it was not mathematically vigorous.

Pretsch,[13] using the method of expansions in terms of small parameters developed by Heisenburg,[3] indicated a method of solving the eigenvalue problem but it is unknown whether he actually made the calculations. His selection of boundary conditions and rejection of certain solutions of the transformed eigenvalue equation causes his approach to the problem to be highly questionable on both mathematical and physical grounds. A detailed criticism of his work has been made by Sellars[11] and Corcos.[12]

The work of Pekeris[10] is considered to be correct but incomplete. He found the eigenvalues of one set of modes whereas two sets of modes actually exist, although he did mention the possibility of two different types of modes.

Sellars,[11] using an analog computer, found a set of modes which were not in agreement with the results of Pekeris. He, therefore, presumed that he had obtained eigenvalues of the other set of modes. This was substantiated by Corcos who found that in addition to the set of modes reported by Pekeris, namely those for which $c \to 1$ as $\alpha R \to \infty$, there exists another set for which $c \to 0$ as $\alpha R \to \infty$. The eigenvalues of the latter set reported by Corcos were slightly inaccurate but in a more recent work by Corcos and Sellars[14] these quantities have been corrected. Their results are believed to be a complete proof of the stability of Poiseuille flow when disturbed by infinitesimal axially symmetric perturbations, since it is shown that c_i is always negative.

The following is a synopsis of the work completed by Corcos and Sellars.[14] It is not intended that this presentation be a complete review of their work but merely a general survey which will enable the reader to gain a greater insight into the philosophy of approach and mathematical pitfalls inherent in the problem.

The differential equation for the eigenfunctions (2.9) has four linearly independent solutions. By using the proper method of approach, it was possible to eliminate two of the solutions which were not sufficiently regular near the center of the pipe.

Following a procedure used by Sexl[8] and Pekeris,[10] the expression for the undisturbed velocity profile is given in nondimensional form as $U(r) = 1 - r^2$. Substitution of this expression into (2.9) gives

$$f'' - \frac{1}{r} f' - \alpha^2 f - i\alpha R(1 - r^2 - c)f = 0 \qquad (2.11)$$

where

$$\phi'' - \frac{1}{r} \phi' - \alpha^2 \phi = f \quad . \qquad (2.12)$$

Noting that $f = 0$ is a solution of (2.11), hence solutions of

$$\phi'' - \frac{1}{r} \phi' - \alpha^2 \phi = 0 \qquad (2.13)$$

satisfy (2.9), and the so-called inviscid, or perfect fluid solutions are obtained. They are referred to as inviscid solutions because they are obtained by letting $R \to \infty$ in the perturbation equation (2.9). Two linearly independent solutions of (2.13) are obtained but due to nonconformity with the boundary conditions at the origin (center of the pipe) one must be rejected leaving only

$$\phi_i = r\, J_1(i\alpha r) \quad . \qquad (2.14)$$

The second set of linearly independent solutions is referred to as the viscous solutions and is assumed to be of the form

$$\phi_a = e^{g(r)} \quad . \qquad (2.15)$$

It is assumed that for large αR an asymptotic series can be used to describe g, namely,

$$g = (\alpha R)^n g_0 + g_1 + (\alpha R)^{-n} g_2 + \ldots\ldots \quad . \qquad (2.16)$$

Substituting (2.15) and (2.16) in (2.9) and equating proper terms we get

$$n = 1/2, \; g_0 = \pm \int_{r_0}^{r} \sqrt{i\alpha(U-c)}\, d\rho, \; g_1 = \log \frac{r^{1/2}}{(U-c)^{5/4}} . \qquad (2.17)$$

Using only the first and second terms of (2.16) an approximation of the

solutions is obtained, namely,

$$\phi_a = \frac{r^{1/2}}{(U-c)^{5/4}}\left[A\, e^{\int_{r_o}^{r}\sqrt{i\alpha R(U-c)}\,d\rho} + B\, e^{-\int_{r_o}^{r}\sqrt{i\alpha R(U-c)}\,d\rho}\right]. \qquad (2.18)$$

The ratio A/B is determined by comparing ϕ_a with a regular (viscous) solution valid in the neighborhood of $r = 0$. It is found to be $A/B = i$. This ratio is not expected to remain constant for the whole interval, $0 \leqq r \leqq 1$, particularly in the neighborhood of the singularity $U = c$ because the asymptotic representation must be single valued if it is to approximate an exact solution of (2.9).

It was noted that the coefficients of A and B had branch cuts and were multivalued functions of r, where r was complex. This led to the result that either A or B must be modified when entering different regions of the complex r plane if the representation was to be continuous. This property is known as the Stokes' phenomenon. The regions that yielded valid solutions were determined by investigating whether the eigenvalues obtained were consistent with the assumptions.

This analysis led to a rather complicated algebraic eigenvalue equation which determined c as a function of α and αR. The equation could be solved by a trial and error process only; however, conclusions could be noted by considering the general behavior of the eigenvalues and examining the limiting cases, namely, $c \to 1$ as $\alpha R \to \infty$ and $c \to 0$ as $\alpha R \to \infty$.

In the first limiting case a family of eigenvalues given by

$$c = 1 + \frac{4N}{(\alpha R)^{1/2}}\, e^{-\frac{3\pi i}{4}}; \quad N = 1,2,3, \ldots. \qquad (2.19)$$

was obtained. This family contains values of c that correspond to damped disturbances only. The use of (2.19) is restricted in the sense

that a relatively small number of modes is given accurately since $4N$ must be much smaller than αR.

The second limiting case gave a family of eigenvalues described by

$$c = \frac{1}{2(2i\alpha R)^{1/3}}\left[3\pi\left(4N + 1 - \frac{4\theta}{\pi}\right)\right]^{2/3}; \quad N = 0,1,2, \ldots.$$

where

$$\theta = \arctan\left[\frac{\sqrt{2}}{5}\,(2i\alpha R)^{1/2} c^{3/2}\right]. \tag{2.20}$$

This again corresponds to damped disturbances. The value of N must again be restricted. Here N must be limited to values such that $|c| \leq 1$.

An investigation was made to determine whether the asymptotic representations leading to (2.19) and (2.20) were valid when $R \to \infty$. The question arises because the singularity, $U = c$ (Stokes point) approaches the boundaries of the interval, namely $r = 0$ in the case of (2.19) and $r = 1$ in the case of (2.20) as $R \to \infty$. It was shown that (2.19) gives a family of eigenvalues which are correct. In fact, a greater number of modes will be given with greater accuracy when R increases. In the case of (2.20) however, the accuracy of the solution is greatly impaired when the Stokes point approaches $r = 1$. Using some of Lin's[7] results an alternate approach was developed to give a more accurate viscous solution. This analysis resulted in a determination of the eigenvalues in terms of the Tietjens function, $F(z)$, where for Poiseuille flow

$$z = (1 - \sqrt{1 - c})(1 - c)^{1/6}\, 2^{1/3}(\alpha R)^{1/3}. \tag{2.21}$$

From this an equation was developed which gave a discrete set of values for z, called z_n, which lie in pairs and are very nearly reflections about the line $\arg z = -\pi/6$. Employing a method of numerical integration

various pairs were computed. The least stable solution was found to be given by

$$z_1 = 4.23\, e^{-\frac{\pi i}{12}} \tag{2.22}$$

which comes from the pair

$$z_{1,2} = 4.23\, e^{i\left(-\frac{\pi}{6} \pm \frac{\pi}{12}\right)} . \tag{2.23}$$

Combining (2.21) and (2.22) the first mode of the second set of eigenvalues is given by

$$4.23\, e^{-\frac{\pi i}{12}} = (1 - \sqrt{1 - c})(1 - c)^{1/6} 2^{1/3} (\alpha R)^{1/3} \tag{2.24}$$

which can be solved for c by trial and error for a particular value of αR.

It was also shown that at each end of the interval, $c = 0$ to $c = 1$, there are a finite number of eigenvalues described by z_n and (2.19). In the middle region where the two modes join, however, neither representation is accurate, and therefore the complete algebraic eigenvalue equation must be used. The present solutions however indicate that only a finite number of eigenvalues exist for any value of αR.

Figures 2 and 3 were supplied by Corcos and Sellars.[14] These figures show the results of their numerical calculation and analog computer results. Figure 2 illustrates the values of c given by (2.19) and (2.20) and by various pairs of z_n at $\alpha R = 10{,}000$. Figure 3 gives the comparison between their computer results and (2.24) in terms of c_r and c_i vs $(\alpha R)^{1/3}$.

It should be noted that the theory has several limitations. First of all, its use must be confined to cases involving small disturbances. However, no accurate criteria is provided to establish the maximum allow-

able amplitude of a small disturbance. Secondly, while it predicts stability to small disturbances, the introduction of large disturbances results in transition to turbulent flow and no explanation of the mechanism is included. Thirdly, stability is predicted for all values of αR; however, it seems reasonable to expect that there is some upper limit to αR in the practical case.

EXPERIMENTAL APPARATUS AND PROCEDURE

(a) EXPERIMENTAL APPARATUS

The experiments were conducted in a lucite pipe 1.25 inches in diameter and 73 feet (700 diameters) long. The air was supplied from a high pressure tank, passed through a settling chamber and discharged through the pipe to the atmosphere. Figure 4 is a schematic diagram of the equipment.

High pressure air (90 psi) from the laboratory supply line was passed through a separator to remove most of the oil and water present in the incoming air. From the separator the air proceeded through an activated alumina dryer to a pressure regulating valve which controlled the pressure in a 100 cu ft storage tank used as a constant pressure source for the air supply system. Air flowed from the tank through a flowmeter to the settling chamber for the pipe. The flowmeter was used simply as a monitor to detect any change in Reynolds number during a run. High pressure rubber hose was used as the supply line between the pressure tank and the settling chamber. The air flowed into the settling chamber through a length of straight pipe in which was mounted a honeycomb to remove swirl and secondary flows introduced by pipe elbows located at its upstream end. Also a coarse screen was placed in the pipe to help remove large scale disturbances in the air supply. In addition, two relatively coarse screens were placed at the inlet to the settling chamber to inhibit the initiation of separation at that point. In the settling chamber two baffle plates were placed opposite the inlet to help remove any jet effect which might result in nonuniform flow. Downstream of the baffles, two relatively coarse screens, a fine screen, a honeycomb and three fine screens were

mounted in that order. The relatively coarse screens were 50 mesh, and the fine ones 100 mesh. The honeycomb cells had a 6:1 length to width ratio. Following the last screen was a wooden nozzle having a 64:1 contraction ratio. Air flowed from the nozzle into the lucite pipe. Figure 5 is a photograph of the experimental setup.

The settling chamber design proved to be satisfactory. No transition to turbulent flow occurred within the pipe at any flow rate within the range of the system. In fact, at one point in the preliminary investigations the inlet to the settling chamber was partially blocked by a piece of sheet metal covering one-half the inlet cross section. This had no measurable effect upon the shape of the fully developed laminar profile at the downstream end of the lucite pipe. Figure 6 is a photograph of the settling chamber.

Uniformity of the internal diameter and concentricity of the pipe, as supplied by the manufacturer, were found to be within 0.005 inch for all sections of pipe used. The length of each section was approximately 50 inches. To insure against any discontinuity of the inner wall of the pipe at the junctions of adjacent sections, the ends of each section were accurately machined and bolted together by means of flanges cemented to the outer surface. In order to eliminate any adverse effects due to curvature along the length of the pipe, a theodolite was used to align and level the pipe. Alignment was accomplished by locating the theodolite beyond the exit of the pipe; then, starting at the upstream end, each section was aligned as it was added until the entire pipe was assembled (see Fig. 5). It was estimated that this method of alignment resulted in a system which departed at most only several hundredths of an inch from true alignment over the entire length of pipe.

All measurements were made by means of a hot-wire anemometer. The associated switching and electronic equipment, Fig. 7, consisted of a Thiele-Wright hot-wire anemometer system, a dual-beam cathode-ray oscilloscope, a Polaroid-Land camera and several oscillators. All signal outputs were mean-square values obtained from a thermocouple located at the output of the hot-wire signal amplifier. Mean velocity measurements were obtained by means of the Wheatstone bridge and the potentiometer of the Thiele-Wright equipment. All hot-wire anemometers were calibrated by using a free jet of air, a pitot-static tube and a Betz-type micromanometer.

Figures 8 and 9 are photographs of one of the two hot-wire probe assemblies used to make radial surveys inside the pipe. Accurate positioning of the hot-wire probe along a diameter of the pipe was achieved by means of the micrometer gage. Azimuth positioning was accomplished by merely rotating the entire assembly about the axis of the pipe. Figure 10 shows a probe installed in the pipe. It was estimated that all radial position readings were accurate to within five thousandths of an inch. The correspondence between gage reading and probe position was determined by moving the probe until the hot-wire just touched the wall of the pipe and then noting the gage reading.

The hot-wire element itself was a platinum wire approximately one millimeter long and 0.0002 inch in diameter. This element was made from Wollaston wire, the platinum core being covered by a silver sheath. The hot-wire element was attached to the probe in the following manner. First, a length of Wollaston wire was formed into a U, the ends of which were soft soldered to the needles of the probe. The shape and size of the loop was determined by the length and tension desired in the final hot-wire

element. The silver sheathing was then removed electrolytically by means of a small jet of very dilute nitric acid and a small electric current. The jet was utilized to obtain uniformity in resistance of the hot wires by controlling the length of etched wire. When the silver sheathing was removed, exposing the platinum wire, tension in the loop caused it to open slightly drawing the platinum into a straight line. A straight wire is essential for accurate measurements.

To take measurements at a fixed radial distance from the wall and in a longitudinal direction, a probe was constructed in such a way that it could be made to slide along the wall of the pipe. This probe is shown in the foreground of Fig. 8 and shall be referred to as the "bug." By means of the "bug," measurements of signal amplitudes and phase angles, as a function of distance along the pipe, could be made.

The disturbance generator, Figs. 11 and 12, was an electromagnetic device which introduced velocity fluctuations into the flow within the pipe. Figure 13 is a schematic cross-sectional view of the generator. The motive element consisted of a coil located in a permanent magnetic field. When excited by an alternating current a sinusoidal oscillation, parallel to the axis of the pipe, was imparted to the coil. Amplitude of the motion at a given frequency was varied by varying the driving current. The range of frequencies within which the generator operated satisfactorily was from approximately zero to 150 cps. Attached to the coil was a cylindrical sleeve having a wall thickness of 0.002 inch and a length of two inches. When in position the sleeve formed a section of the inner wall. Disturbances were imparted to the uniform flow through the action of friction between the sleeve and the adjacent flow field. Motion of the sleeve altered the boundary conditions at the wall and therefore super-

imposed disturbance velocities upon the axially symmetric parabolic flow field.

The above method produced disturbances which were not completely axially symmetric. Another attempt to produce axially symmetric disturbances and at the same time obtain larger velocity perturbations was made by centrally mounting a ring airfoil within the cylindrical sleeve. The airfoil had a chord of 0.10 inch and a thickness of 0.003 inch. The diameter of the ring was approximately 0.9 inch and was a truncation of a cone having a cone angle of six degrees.

(b) EXPERIMENTAL PROCEDURE

After assembling and aligning the pipe, measurements of velocity profiles were made at several stations along the pipe for various Reynolds numbers. These radial surveys revealed that the undisturbed velocity distribution was not axially symmetric, the maximum velocity of the parabolic distribution occurring below the centerline of the pipe. A systematic reorientation of the various components of the settling chamber and pipe plus a modification of the settling chamber inlet effected no change in the velocity distribution. It was decided that the asymmetry was not due to any geometric configuration but rather to some more subtle phenomenon.

Several radial surveys near the pipe inlet indicated that the dissymmetry was actually originating within the settling chamber by showing that the velocity of the core was not uniform but was slightly greater near the bottom of the pipe. Radial surveys of temperature and velocity distribution were made within the settling chamber but the results were inconclusive because of vibration of the probe near full extension and the minuteness of variations in the radial distributions of these quantities. Maximum temperature and velocity differences across the settling

chamber were approximately 0.4 degree centrigrade and 0.04 foot per second, respectively. These were of the same order of magnitude as the respective sensitivities of the system. Therefore, a heating element was placed at the upstream end of the settling chamber near the baffle plates, as shown in Fig. 4. The purpose was to create a temperature gradient within the settling chamber and note the effect upon the fully developed laminar profile. The curved heating element, made from a length of pyrex glass tubing with a nichrome wire wound around it, spanned a central angle of approximately 150 degrees. At first the element was located in the bottom sector of the annulus. As the heat was gradually increased, no noticeable effect was detected until above a critical value of the heating current the flow within the pipe became turbulent. Upon reducing the heat the flow returned to the laminar state. It seemed apparent that the temperature gradient artificially introduced within the settling chamber by the heater in that position had a very severe destabilizing effect, so it was relocated diametrically opposite, at the top of the settling chamber.

Placing the heating element in the top sector of the annulus proved to be the solution of the problem. By correctly adjusting the heating current the maximum velocity of the parabolic distribution could be positioned at the center of the pipe. If the current were increased or decreased from the correct value, the position of maximum velocity would move upward or downward, respectively.

A number of fully developed velocity profiles were obtained at various Reynolds numbers. The stations along the pipe at which these profiles were obtained corresponded to stations at which the disturbance generator was placed when runs were made at corresponding Reynolds numbers. Several

of these velocity profiles are given in Figs. 15 and 16. It can be seen that good agreement between experiment and theory was obtained by the addition of heat. A velocity profile obtained when no heat was added is shown in Fig. 14.

Before any series of runs was to be made the profile was checked by determining whether the point of maximum velocity coincided with the centerline of the pipe. If its location was off the centerline the heat was adjusted to effect coincidence.

After a symmetrical profile was obtained, the disturbance generator was fitted into place and hot-wire probes were placed downstream of it. Preliminary surveys were made to determine the range of disturbance frequencies which appeared to be the least stable, i.e., those for which the exponential damping factor was the smallest. Then radial surveys of the disturbance were made at several stations downstream of the generator.

To observe whether the signal level varied during a run, a monitor hot wire was used. This hot wire could not be placed immediately behind the disturbance generator because its wake altered the disturbance configuration in the test regions. Therefore, in each case the monitor hot wire was located in the test region and diametrically opposite the test probe.

The procedure for making measurements by means of the "bug" was the same as above. The generator was operated at constant amplitude while the "bug" was moved longitudinally along the pipe. A monitor probe was located near the opposite wall of the pipe. The purpose of these measurements was to obtain the wave length and decay rate of the disturbance as a function of Reynolds number and frequency. The terms computed from these quantities allow the experimental results to be compared with the theory.

All radial surveys were begun at the wall. The probe was moved inward and the "bug" longitudinally in steps that were considered adequate to give consistent results. At each radial and longitudinal position the Wheatstone bridge was balanced so that the hot wire had the same mean resistance for all measurements and therefore operated at the same overheating ratio.* The signal output was read on a millivoltmeter which was actuated by the output of a thermocouple. The thermocouple in turn was energized by the hot-wire signal amplifier. Readings obtained by this method were mean-square values. After the signal amplitude was obtained, the disturbance generator was stopped and the mean-square value, which was interpreted as the "noise level," was taken. It was assumed that the disturbance signal and the noise were uncorrelated, and hence the mean-square quantities could be subtracted directly, yielding the signal amplitude alone.

The mean-square signal amplitude was referred back to the amplifier input - the hot-wire output - by means of an amplifier calibration procedure. After each series of runs the amplifier was calibrated at each gain setting used in the runs by means of an oscillator. To obtain disturbance velocities from the fluctuating voltages appearing across the hot wire, a conversion factor had to be used. This factor is a function of the local mean velocity, average resistance of the hot wire and the average current flowing through it, the overheating ratio, the static hot-wire calibration and various circuit constants. For further information concerning hot-wire sensitivity and compensation see reference 15.

*No hot-wire compensation was used because the frequency range of the disturbance signals was within the region of flat frequency response of the hot wire.

Phase angles were measured on the face of a dual beam cathode-ray oscilloscope. The common reference signal used for all phase angle measurements was the input voltage to the disturbance generator. By putting this signal on one beam of the oscilloscope and the hot-wire signal on the other beam, relative phase angles could easily be determined with an accuracy of approximately $\pm$ 5 degrees.

SUMMARY OF RESULTS

A velocity profile without heat addition in the settling chamber is shown in Fig. 14 and profiles, taken in the testing region at Reynolds numbers of 4,000, 6,600 and 13,000, with heat addition are given in Figs. 15 and 16.

Typical peripheral surveys of the disturbance at radial positions $r/a = 0.808$, 0.648 and 0.488 are shown in Fig. 17. Comparison between surveys at stations 5.6 and 12.4 diameters downstream of the disturbance generator are presented.

Radial distributions of disturbances taken at several stations along the pipe and at the three testing Reynolds numbers are shown in Figs. 18 to 32. The local root-mean-square velocity ratios are given in Figs. 18 to 24 and the relative phase angles in Figs. 25 to 32. A pictorial representation of the radial disturbance distribution at a frequency of 40 cps and a Reynolds number of 4000 is given in Fig. 33. The top trace in each picture is the reference signal obtained from the driving voltage supplied to the disturbance generator. Perturbation velocity increases are indicated by upward deflections of the bottom trace.

Results of longitudinal surveys taken at $r/a = 0.76$, frequencies of 25, 35, 40 and 45 cps and Reynolds numbers of 4,000 and 13,000 are given in Figs. 34 to 37. Figures 34 and 35 give the logarithmic decrease of the root-mean-square velocity and Figs. 36 and 37 show the linear variation of the relative phase angles with increasing distance downstream.

Comparison between theory, Equation (2.24), and experiment is shown in Fig. 38 where c_r and $-c_i$ are plotted against $(\alpha R)^{1/3}$.

Figure 39 gives the variation of c_r with r/a at several stations and

Reynolds number of 4,000 to 13,000. Plots of $r\, c_{r/a}$ vs r/a at several frequencies and Reynolds numbers of 6,600 and 13,000 are given in Fig. 40. A cross plot of $r\, c_{r/a}$ vs x/d is given in Fig. 41.

Figure 42 is a pictorial representation of transition from laminar to turbulent flow through the mechanism of distortion of the disturbance caused by small increases in the amplitude of the disturbance generator. The top trace represents the voltage input to the disturbance generator and provides an indication of the relative amplitudes of the initial disturbance. Perturbation velocity increases are indicated by upward deflections of the bottom trace.

Radial measurements at several stations of turbulent diffusion behind the ring airfoil were made at a Reynolds number of 12,000. Figure 43 is a plot of u'/U_{max} vs r at each station and Fig. 44 gives the mean velocity profiles. Results obtained at the last station are compared with the results Laufer obtained at a Reynolds number of 50,000.

DISCUSSION

(a) UNDISTURBED FULLY DEVELOPED LAMINAR FLOW

The attainment of undisturbed laminar flow for all flow rates up to the maximum capacity of the system, approximately R = 20,000, was achieved with no difficulty. The initial precautions of adequate damping screens in the settling chamber, a well-rounded inlet to the pipe, and a straight pipe with smooth joints proved to be sufficient. However, the procuring of axially symmetric, fully developed velocity profiles was an arduous task.

After making every feasible geometrical alteration to the system with negative results, an asymmetric heating (see Fig. 4) of the air at the upstream end of the settling chamber produced an axially symmetric profile. A velocity profile without heating is shown in Fig. 14; the approximately symmetrical profiles of Figs. 15 and 16 show the effect of heating. The amount of heating current necessary to retain a symmetrical profile appeared to be not only a function of the Reynolds number but also of the ambient temperature of the laboratory, which undoubtedly was reflected in the temperature of the air in the storage tank. In general, the higher the ambient temperature the larger the heating current required. The relationship between heating current and Reynolds number was rather difficult to determine because of the ambient temperature relationship. In general, it appeared that the higher the Reynolds number the smaller the heating current required, though the differences were not large. The relation between heating current and ambient temperature was quite pronounced especially when the latter changed appreciably during the day. With the system operating at a constant Reynolds number and the heating current held constant, the maximum velocity would be above the centerline of the

pipe in the morning and below in the afternoon after the laboratory became heated by the sun. Therefore, on such days the heating current had to be continuously increased to maintain an axially symmetric velocity profile.

The average amount of heat added was approximately ten watts. Assuming half the air passing through the settling chamber was heated, the addition of that amount of heat corresponds to a temperature rise of 2.3 degrees centigrade at R = 13,000. Beyond these qualitative observations no further investigations concerning the asymmetric phenomenon were made because such work lay outside the scope of the present problem.

Small flow variations, with a period of several minutes, caused the maximum velocity point to wander slightly about the centerline of the pipe. It was thought that these variations were due to ambient air disturbances propagating upstream from the exit of the pipe. Such distrubances may be pressure fluctuations caused by large scale eddies induced by the ventilation system in the laboratory.

In addition to the above distrubances, extremely small, relatively high frequency disturbances formed a noise background in the flow. The amplitude appeared to be somewhat sensitive to Reynolds number but had a maximum value of u'/U of approximately 0.01 percent. The greatest portion of the noise was believed to be sound because the amplitude remained roughly constant across the pipe.

Lengths of transition for several Reynolds numbers were checked approximately and compared with the calculated results of Boussinesq.[16] Satisfactory agreement with Boussinesq's formula was obtained at the lower Reynolds numbers. At higher Reynolds numbers, however, his formula gave lengths of transition which appeared to be too large. Figure 16 shows

that at R = 13,000 agreement with theory was good even though the Boussinesq formula indicates that the measurement location is only 0.8 of the inlet length.

The small discrepancies between experimental and theoretical profiles near the walls may be due to the influence of the hot-wire probe. Tests were made with the supporting stem of the probe spanning the pipe for all probe positions. Results of these tests did not differ measureably from results obtained when the stem extended only to the hot-wire probe. Of course, in this test the probe itself is still an unsymmetrical disturbance. Regardless of the source, however, the discrepancies did not appear to be large enough to greatly influence the final results.

(b) DISTURBED FULLY DEVELOPED LAMINAR FLOW

On page 9 it was pointed out that recent theoretical investigations indicated that fully developed laminar pipe flow remained stable when disturbed by small axially symmetric disturbances. The mathematical approach to the problem necessitated certain assumptions, which, while being logical and valid mathematically, could not be realized easily in an experimental investigation because of the absence of idealized conditions. Examination of Equation (2.8) describing the type of disturbance assumed to be a solution of the perturbation Equation (2.6), reveals that an initial axially symmetric disturbance, having an identical radial distribution for all values of x, is assumed to be imposed upon the mean flow at each station along the pipe. The initial disturbance is then released and the history of the disturbance as a function of time is then described by the solution. In such a picture the influence of

flow conditions at neighboring stations will be negligible since the disturbance patterns are identical.

Experimentally however, this type of disturbance cannot be imposed due to physical limitations. Actually the disturbance was introduced along the wall at a small number of neighboring stations and propagated radially and longitudinally from there. Due to the fairly rapid decay of disturbances with time, it is rather doubtful that ϕ of Equation (2.8) ever became a function of r alone although Figs. 19 to 24 indicate that this condition was approached. In addition, the continuous decay of the disturbance, as a function of x, meant that amplitudes of the disturbance at neighboring stations were not the same.

The influence of these two differences upon the final results cannot be completely determined. In Fig. 35, the two distinct decay rates may be due to the process by which the disturbance approaches an equilibrium state. The initial decay rate occurs in the region where the radial redistribution of the disturbance takes place as it tends toward an equilibrium configuration. The second rate of decay is much greater and shows satisfactory agreement with the theoretical prediction.

Another source of discrepancy between experimental and theoretical disturbance configurations refers to the axial symmetry of the disturbance pattern. In the theory it was assumed that disturbances were axially symmetric. This disturbance pattern could not be achieved experimentally. Various methods of generating axially symmetric disturbances were attempted but none proved to be completely effective. Deviations of the disturbance from axial symmetry could be caused by any of a number of factors. These are: small deviations of the fully developed flow from axial symmetry, small leaks at the disturbance generator caus-

ing a pumping when the generator is in motion, disturbances at the supports if a disturbance element is supported away from the wall of the pipe, minute departures of the shape of the disturbance element from axial symmetry, and others. All these at some time or other were identified as factors in causing deviations of the disturbance from axial symmetry.

While departures of the disturbances from axial symmetry were troublesome and made measurements more difficult, the comparison with theory is not necessarily invalidated. In fact, complex disturbances may be considered as a superposition of axially and nonaxially symmetric components as long as their amplitude is sufficiently small so that small perturbation theory would be applicable. The nonaxially symmetric component actually would be a three-dimensional disturbance due to its variation with azimuth angle. Squire[17] has shown that, for plane flows, three-dimensional disturbances are more stable than two-dimensional and therefore would decay more rapidly. While the corresponding theorem has not been proved for axially symmetric flow, the peripheral surveys of Fig. 17 seem to indicate that the disturbance has a tendency to become more axially symmetric as it propagates downstream.

(c) MEASUREMENTS OF DISTURBANCES

(1) Peripheral Surveys.—In addition to indicating that the disturbance tended toward axial symmetry, the peripheral surveys of Fig. 17 showed that the disturbances possessed the same general character, as a function of azimuth angle at each station. This fact supported previous measurements which indicated the absence of swirl within the pipe. With this information the making of radial and longitudinal surveys of

the disturbances was simplified because results obtained at various stations could be assumed to be comparable as long as the probe was placed at the same azimuth angle at each station.

(2) Radial Surveys.—In making radial surveys, the ideal situation would have been to place a monitor hot-wire probe close to the disturbance generator so that disturbances having a constant amplitude would have been generated for similar surveys. This was attempted but was abandoned when it was found that the wake from such a probe greatly altered the disturbance pattern. Instead the monitor was placed approximately at the same station that radial surveys were made but diametrically opposite the testing region. This provided a means of maintaining a constant disturbance level during any particular survey but prevented any comparison of disturbance amplitudes obtained from radial surveys at various stations. Attempts were made to maintain a constant signal level by supplying a constant voltage level to the disturbance generator; however, Figs. 18 to 24 indicate that the method was inadequate, possibly because of variations of friction between the sleeve and the pipe wall.

Radial amplitude distributions of disturbances are given in Figs. 19 to 24. In general, all distributions appear to have the same characteristics except near the wall where in some cases a second amplitude peak occurs. More will be said about this later. Since no theoretical determinations of the radial distribution of u' have been made, comparison of these results with theory is not possible. Such calculations have been made for plane Poiseuille flow,[18] but they have not been carried out for pipe flow. Several general comments concerning the physical nature of the disturbance can be made, however. Inspection of the rms amplitude curves reveals that the u-component of the disturbance approaches zero at $r = 0$

and r = a. This is in agreement with the boundary conditions of the mathematical formulation; however, the boundary condition at r = 0 appears to permit the presence of sound waves in addition to shear disturbances, since u is merely constrained to be finite at that point. Such is the case when sound waves are present.

The amplitude curves also indicate the lack of radial equilibrium of the disturbance. Identical initial disturbances have slightly different amplitude distributions at each station. In general, the peak amplitude moves towards the center of the pipe as the disturbances propagates downstream. Figure 23 indicates that the peak amplitude appears to approach an equilibrium position but it is doubtful that equilibrium is achieved before the disturbance is completely dissipated.

No w-component measurements were made because of the difficulty in making an x-wire probe small enough to prevent appreciable interference with the disturbance pattern. Also u-component measurements are sufficient to determine stability characteristics. A pipe having a larger diameter would have to be employed to make accurate w-component measurements.

Relative phase angles of the disturbances are presented in Figs. 26 to 32. The relative magnitudes of the phase angles at the various stations were determined by comparison with "bug" measurements at r/a = 0.76. Phase angles at this radial position were compared with "bug" measurements at the various longitudinal stations so that the total phase shift between stations could be computed and the spacing of the curves determined.

The above curves show that, in all cases tested, the phase angle decreased with decreasing radial position. This indicates that the disturbance was being propagated downstream at a more rapid rate near the center

of the pipe. Apparently the mean velocity profile played an important part in establishing the general characteristics of the disturbance, especially in the central region of the pipe. As will be shown later, the wave velocity at each radial position does not appear to be directly correlated with the mean velocity since the former seems to vary inversely with radial position. Once the disturbance pattern is established, however, the velocity profile appears to exert little influence upon the velocity of propagation. This is illustrated in Fig. 41 where there appears to be no general change in c_r as a function of x.

Several of the curves show a rather abrupt phase shift of approximately 180 degrees. Examination of corresponding amplitude curves, for instance Figs. 21 and 28, will reveal that a velocity minimum also occurs at the same radial position. It appears that this phenomenon indicates the formation of a circulatory disturbance similar to that found theoretically, reference 5, and experimental, reference 6, in stability investigations in boundary layers. The circulatory disturbance appears to be formed near the wall and then propagates radially into the flow as shown in Fig. 28. The mechanics by which this phenomenon takes place are not known. Actually the disturbance pattern is so complex that one cannot say definitely what is happening within the disturbed flow. About all that can be stated is that the complex disturbance introduced experimentally is much more general than the disturbance assumed in the mathematical formulation of the problem. Therefore, the results may not compare directly with theoretical computation because the theoretical results may be simply specialized solutions of the general problem. The results should be reasonably similar, however.

Figure 33 shows the traces which occurred on the dual-beam cathode-

ray oscilloscope during a typical radial survey. The top trace represents the driving voltage supplied to the disturbance generator. This signal provided the common reference for all phase angle measurements. The sweep frequency and horizontal gain were always adjusted so that one cycle extended over 18 divisions on the oscilloscope face thereby providing a horizontal scale of 20 degrees per division. The time scale runs left to right. Relative amplitudes of disturbance are indicated at each radial position.

This series of pictures shows that the phase angle decreased with decreasing r. Also a signal null occurs at $r/a = 0.792$ and is accompanied by a phase shift of approximately 180 degrees. If this phenomenon were a pure circulatory disturbance, the phase angle outside the null region would remain constant as a function of radial position. Hence the additional phase shift, especially near the center of the pipe, indicates that a more complex disturbance is present.

An attempt was made to determine the relationship between c_r and r. To accomplish this, Figs. 26 to 32 were used. By taking differences of relative phase angles occurring at adjacent stations, at the same radial position, c_r was computed for several radial positions. This procedure was carried out for most of the radial surveys that were taken. There appears to be approximately an inverse relationship between c_r and r, Figs. 39 and 40. By cross plotting the above results, Fig. 41 was obtained. This figure indicates that the wave velocity at a particular radial position remains approximately constant as the disturbance propagates downstream.

The above statements can be applied also in the case where the ring airfoil was used as the disturbance element, namely, Figs. 18 and 25.

It should be noted that the disturbance shed from the airfoil was quite different from that introduced at the wall. It contained larger amplitudes and altered disturbance patterns. First of all, this type of disturbance may possess considerably more vorticity since it is actually a wake generated by variation of the lift on the airfoil, and secondly it is introduced at $r/a = 0.72$ and propagates towards both the wall and the center of the pipe. In the few measurements of this disturbance that were taken, it was generally noted that the disturbances were much more regular with no abrupt phase shifts. The range of Reynolds numbers at which this type of disturbance can be employed is quite limited however due to the large ambient disturbance introduced by the presence of the airfoil in the flow field.

(3) Longitudinal Surveys.—Various problems were encountered in obtaining accurate data from the "bug" measurements. First of all, the "bug" had to present a minimum frontal area to prevent appreciable blocking of the flow within the limited confines of the pipe. Secondly, the "bug" had to be moved in such a manner that its orientation remained unchanged, that is, it could not be allowed to wobble or tilt. After considerable adjustment of the "bug" support system a very good set of data was taken at $R = 13{,}000$ and is shown in Figs. 35 and 37. Phase angle measurements, being less sensitive to "bug" orientation than amplitude measurements, were satisfactory in most cases. The amplitudes presented a very erratic distribution when insufficient care was taken, thereby making it extremely difficult to compute damping factors.

Figure 35 shows what was believed to be a phenomenon resulting from nonequilibrium in the radial distribution of the disturbance. The first rate of decay may have been less than the second because of a radial re-

distribution of the disturbance as it tended toward an equilibrium distribution. In both cases the decay rate appeared to be logarithmic. The second rate of decay was used to compute damping ratios which proved to be in satisfactory agreement with theory (see Fig. 38 - circles).

Also in Fig. 35 it should be noted that only a narrow band of frequencies was used. Preliminary tests indicated that the frequency range used provided the best experimental conditions. Frequencies above 45 cps were damped so rapidly that accurate measurements could not be taken while frequencies below 25 cps were difficult to use because of power requirements and difficulties in synchronizing traces on the oscilloscope. Qualitative tests were made at frequencies ranging from 2 to 15 cps. Results indicated damping throughout the entire range.

Figures 34 and 36 were "bug" measurements of the disturbance generated by the ring airfoil. They are quite similar to those mentioned above with the exception that only one decay rate occurred. This may have been due to the fact that the measurements in this case were taken further downstream than in cases of disturbances generated by the sleeve. Also they were made in a region where the local disturbance amplitude was small compared with the maximum amplitude. This can easily be seen by considering the amplitude at r = 0.475 inch in Fig. 18.

(d) WAVE VELOCITY AND DAMPING FACTOR

Wave velocities were determined from curves shown in Figs. 36 and 37 and from similar curves for other conditions. The longitudinal distance the "bug" had to be moved to observe a 360-degree phase shift was called the wave length, λ, of the disturbance. Then by definition the nondimensional wave velocity was given by

$$c_r = \frac{\lambda f}{U_{max}} \quad . \tag{5.1}$$

Figure 38 shows the values of c_r obtained from four separate "bug" measurements. The relatively uniform disagreement with theory at smaller values of αR could be due to the lack of agreement with theoretical disturbance patterns, or to the fact that the disturbance had not approached equilibrium by the time the measurements were taken. The fact that the highest Reynolds number used gave uniformly better agreement may indicate that the type of disturbance generated by the sleeve approaches more nearly the theoretical pattern with increasing velocity gradient at the wall.

Wave velocities associated with disturbances generated by the ring airfoil deviated most greatly from theoretical predictions. This is a further indication that the two disturbances are quite different, and it may show that in the case of the airfoil the amplitudes may have been too large to be in agreement with small perturbation theory. Also the "bug" measurements were not made in the region near the maximum disturbance.

The values of damping factor c_i were obtained from the slopes of curves similar to those shown in Figs. 34 and 35. In accordance with Equation (2.5) the u-component of velocity can be written as

$$u = -\frac{\phi'(r)}{r} e^{\alpha c_i t} e^{i\alpha(x-c_r t)} . \qquad (5.2)$$

The change in amplitude with respect to time can be expressed, using (5.2) as follows:

$$\frac{u_2}{u_1} = e^{\int_{t_1}^{t_2} \alpha c_i \, dt} . \qquad (5.3)$$

In Fig. 34 x_o denotes a position 26.4 diameters downstream from

the ring airfoil and in Fig. 35 x_o corresponds to position 3.6 diameters downstream from the sleeve. In both figures, u'_o is the rms amplitude at x_o and u' the amplitudes at stations downstream of x_o.

Writing Equation (5.3) in terms of the measured quantities we get

$$\frac{u'}{u'_o} = e^{\int_{t(x_o)}^{t(x)} \alpha \, c_i \, dt}$$

or

$$2.3 \log_{10} \frac{u'}{u'_o} = \int_{t(x_o)}^{t(x)} \alpha \, c_i \, dt \quad .$$

Differentiating with respect to t and using relation $dx/dt = c_r$ this equation then becomes

$$c_i = \frac{2.3 \, c_r}{\alpha} \frac{d}{dx} \left(\log_{10} \frac{u'}{u'_o} \right) \quad . \tag{5.4}$$

The computation of c_r was shown above. Hence if changes of u'/u'_o with respect to x are the result of damping of the disturbance, the slopes of the curves should enable c_i to be computed by Equation (5.4).

Satisfactory agreement with theory is indicated in Fig. 38. Some of the scatter of the points was believed to be due to imperfect tracking of the "bug" which resulted in rather erratic amplitude representations.

Again the data obtained from disturbances created by the ring airfoil deviated most greatly from theoretical predictions. The fact that the damping factors for these disturbances are much smaller than predicted could be interpreted as an indication that the disturbance amplitudes were too large. As is indicated by the results and discussion in the next section, the flow becomes less stable as the amplitude of disturbance was increased until finally transition occurs.

(e) TRANSITION INDUCED BY LARGE DISTURBANCES

With the hot-wire probe located at r/a = 0.568 and 47 diameters downstream of the ring airfoil, which was oscillating at 25 cps, and with R = 4000 the series of pictures shown in Fig. 42 was obtained by gradually increasing the amplitude of oscillation. Again only u-components of velocity were observed. The top trace is the input voltage to the disturbance generator and time is measured from left to right. The bottom trace is the signal from the hot-wire probe where upward deflections correspond to velocity increases.

A result of this test is that the onset of turbulent flow is not an instantaneous phenomenon but a process of distortion of the imposed disturbance. Each picture gives a reproducible state of the disturbance and not merely a transient condition. The process was reversible in the sense that it repeated, regardless of the direction of approach to any of the states, that is, from low to high or high to low disturbance amplitudes.

In Fig. 42 the imposed disturbance amplitude is represented by the amplitude of the top trace. For convenience, the amplitude of the input signal, in terms of divisions on the oscilloscope grid, is given with each picture. Also accompanying each picture is the ratio of the particular rms velocity fluctuation to the maximum rms fluctuation, shown in exposure no. 3.

It has been shown previously that small disturbances decayed in all cases investigated. The introduction of large disturbances, however, led to instability. Somewhere between these two amplitude extremes must be an amplitude which is nearly neutrally stable. Tests made with the same disturbance element as above, at R = 8000, showed that transition was induced when the airfoil was oscillated with the smallest possible amplitude.

At R = 12,000 the ring airfoil, when in a stationary state, introduced disturbances which appeared to be completely turbulent for all practical purposes. When radial traverses were made at several stations downstream of the airfoil, the turbulent wake appeared to diffuse uniformly in a radial direction and the fluctuations increased in amplitude.

Figure 43 gives the nondimensional disturbance distribution while Fig. 44 gives the corresponding mean-velocity distribution at several stations downstream of the ring airfoil. It should be noted that the disturbances originated immediately behind the ring airfoil which had a mean radius of 0.45 inch.

Results of the traverse at station 47 are compared with the results Laufer[19] obtained in fully developed turbulent pipe flow at R = 50,000. The comparison indicates that the flow is very nearly in the turbulent state. The mean velocity and fluctuating velocity distributions agree quite well in spite of the difference in Reynolds number.

The significance of the above qualitative results should be emphasized again. The onset of turbulence in fully developed laminar pipe flow is not an abrupt phenomenon. There is a process by which disturbances having a sufficiently large amplitude will grow until the fully turbulent state is established. Also the introduction of turbulent spots, or rings in this case, will lead to fully turbulent flow but only through a mechanism which appears to be a continuous transition process. It appears that the maximum allowable amplitude for the preservation of stability decreases with increasing Reynolds number.

CONCLUSIONS

1. Axially symmetric, fully developed laminar flow in a pipe is stable to small disturbances, whether they are axially symmetric or not, up to R = 13,000. This conclusion is based on the observation that nonaxially symmetric disturbances decay at least as rapidly as axially symmetric disturbances.

2. Experimental values of rate of decay and of speed of propagation of the disturbances are in satisfactory agreement with theoretical predictions.

3. Some dependence of speed of propagation of the disturbance on radial position was found. The theory does not postulate any relationship between wave velocity and radius; therefore, no comparison could be made.

4. Instability and transition to turbulent flow are excited when the disturbance exceeds a given amplitude. This maximum amplitude of disturbance for the preservation of stability decreases with increasing Reynolds number within the range of the experiments.

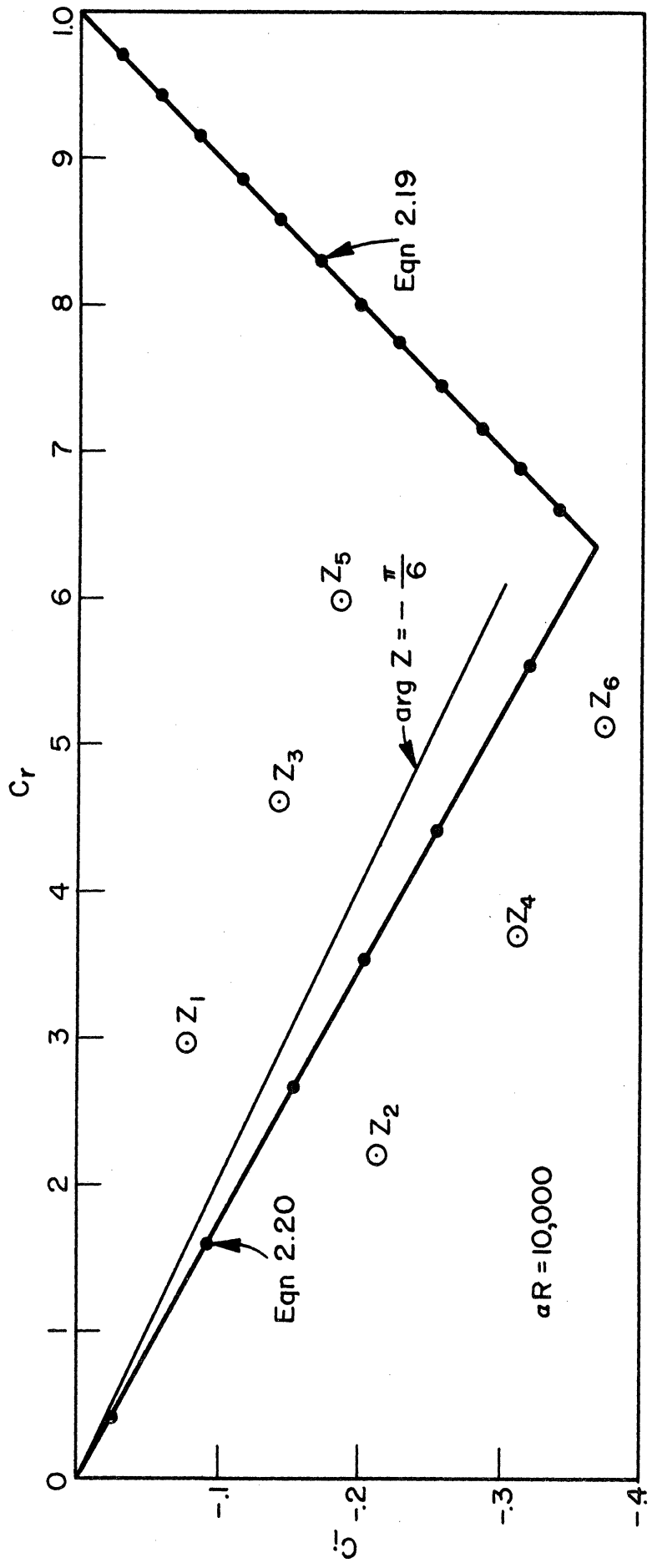

Fig. 2. Theoretical eigenvalues.

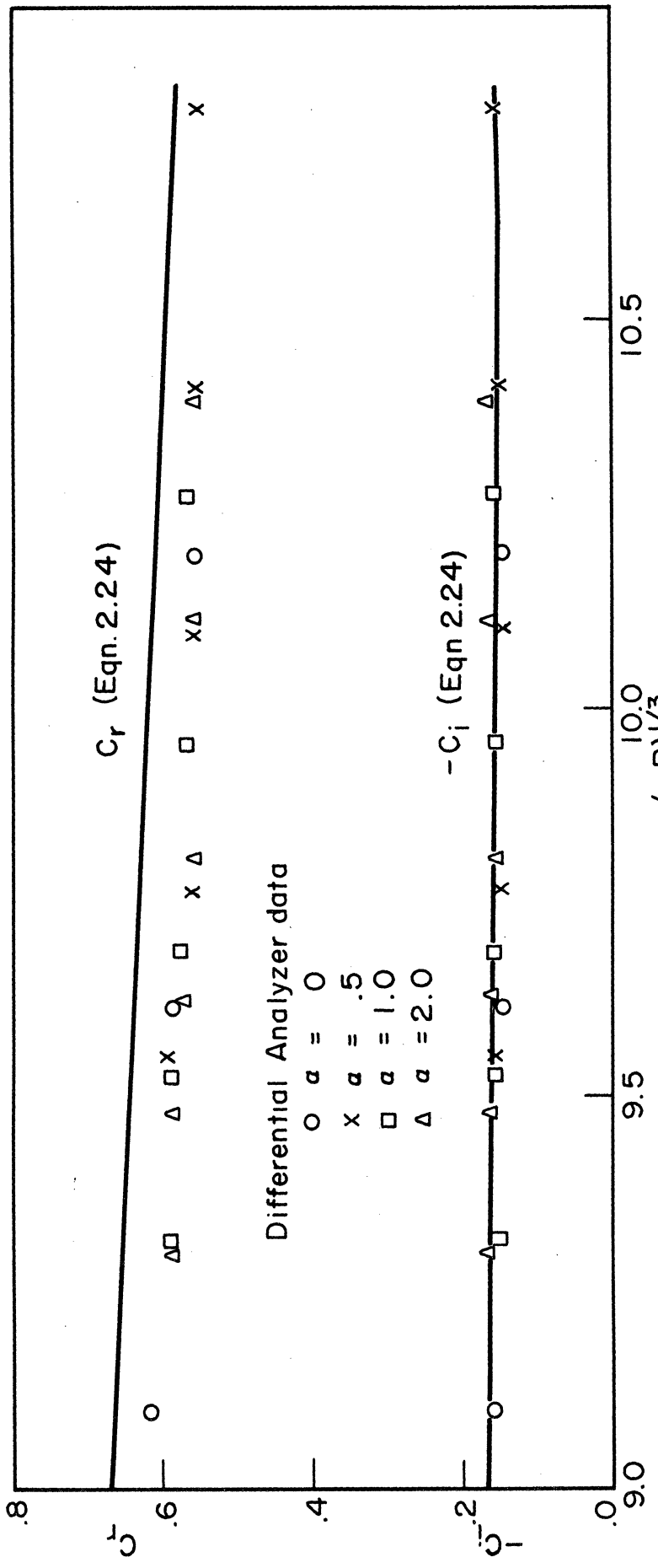

Fig. 3. c_r and $-c_i$ vs $(\alpha R)^{1/3}$ (computer results).

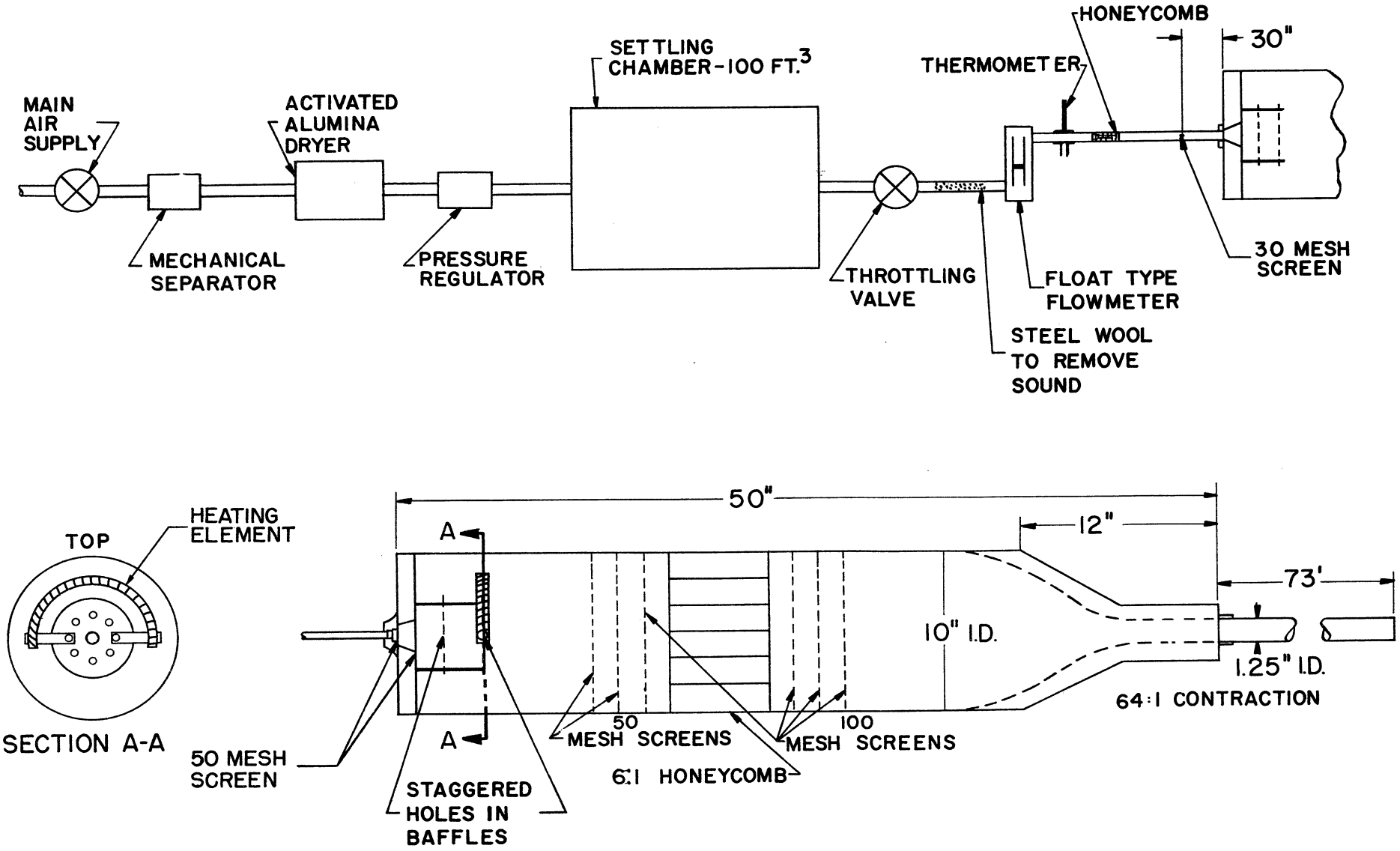

Fig. 4. Schematic diagram of air supply system.

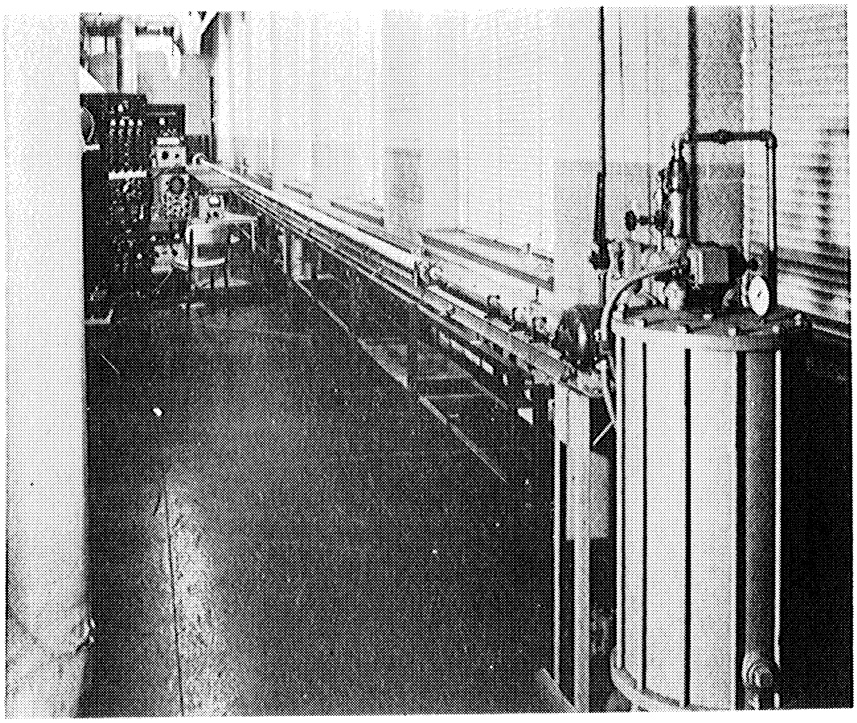

Fig. 5. Photograph of experimental apparatus.

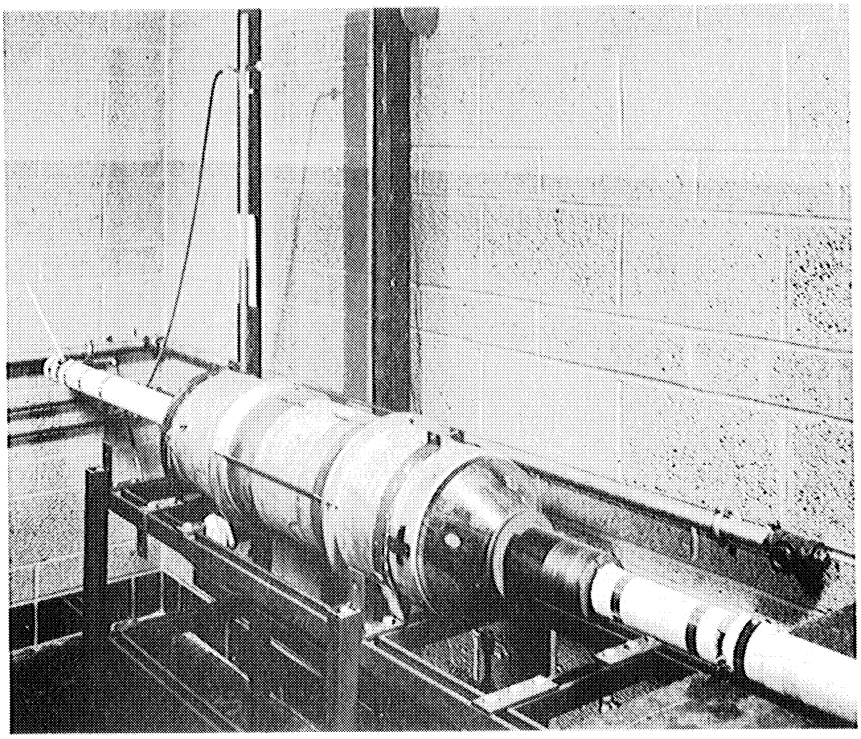

Fig. 6. Photograph of settling chamber.

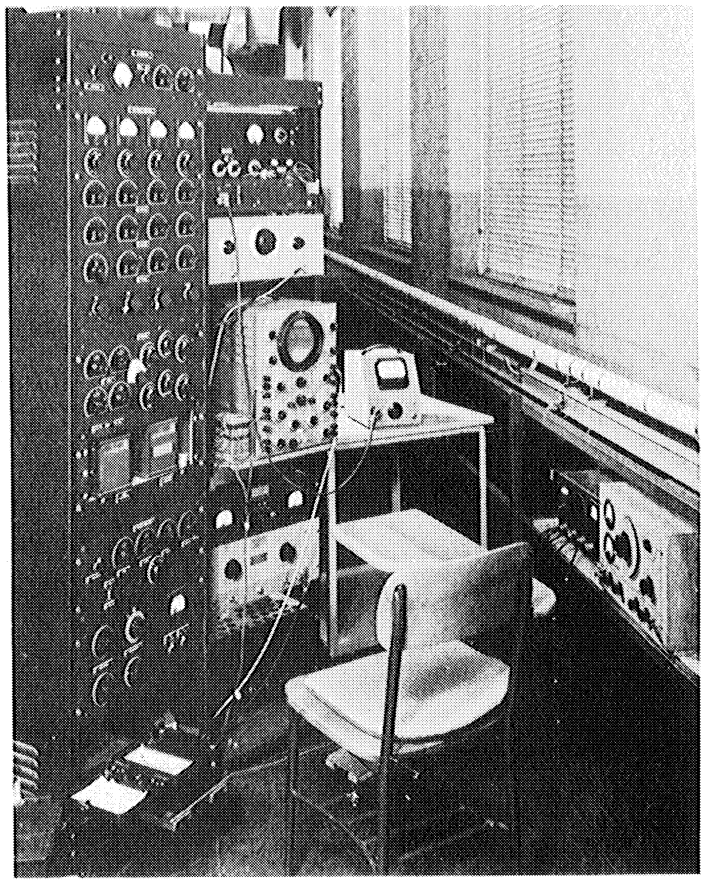

Fig. 7. Photograph of electronic equipment.

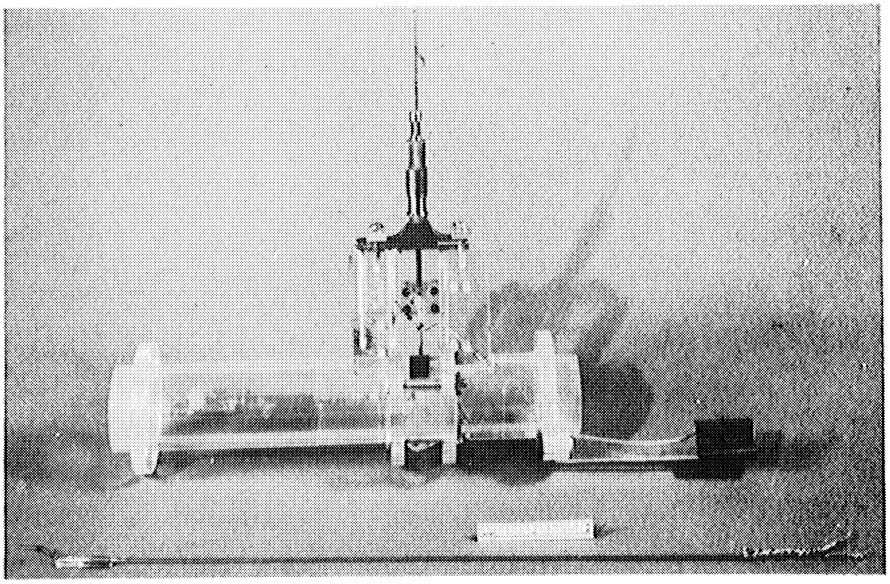

Fig. 8. Photograph of hot-wire probe and "bug."

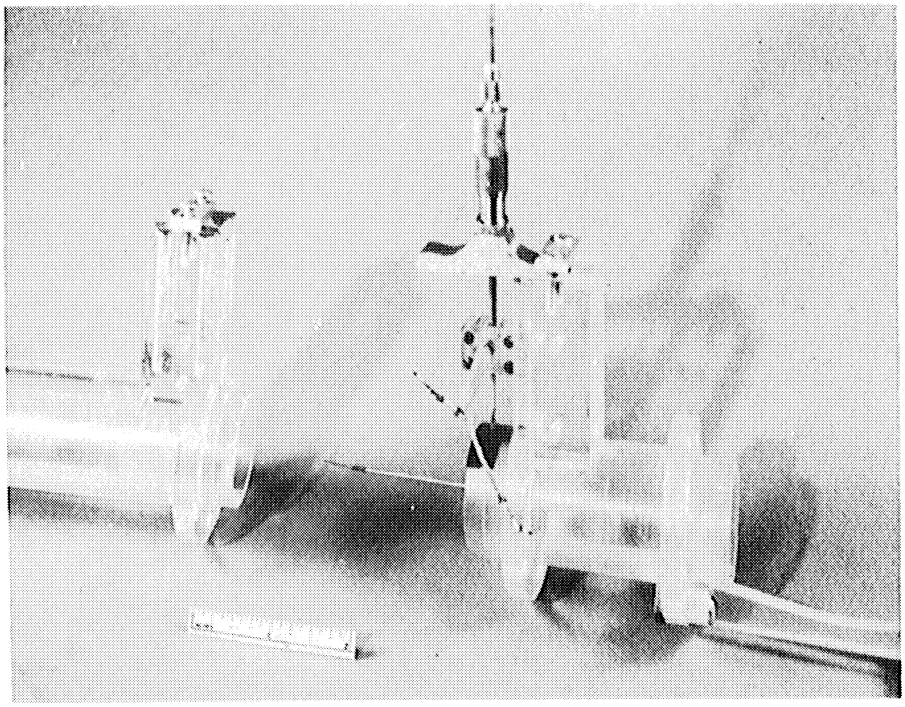

Fig. 9. Photograph of hot-wire probe (exploded).

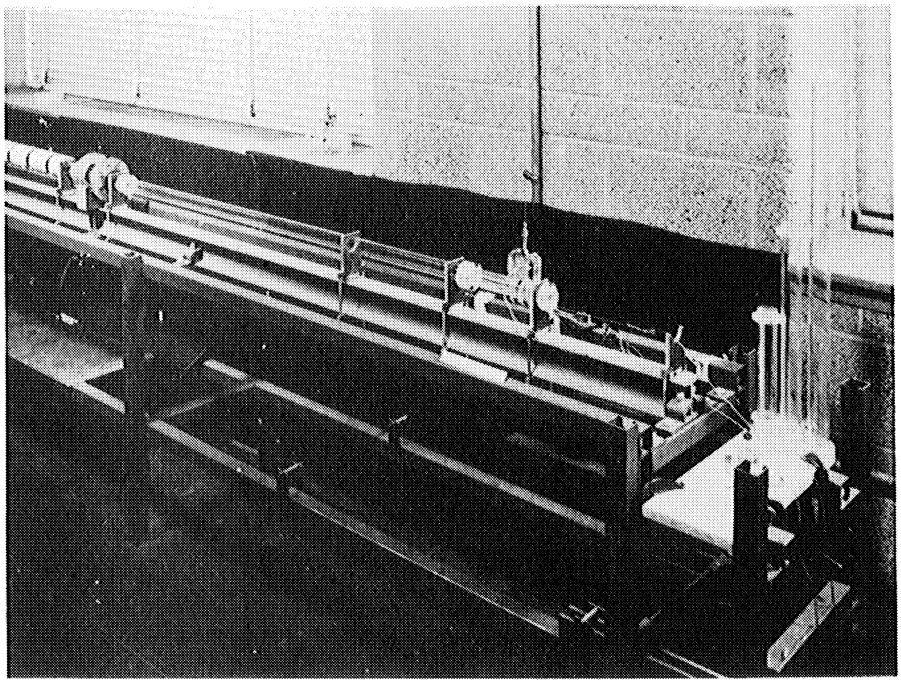

Fig. 10. Photograph of hot-wire probe installed in the pipe.

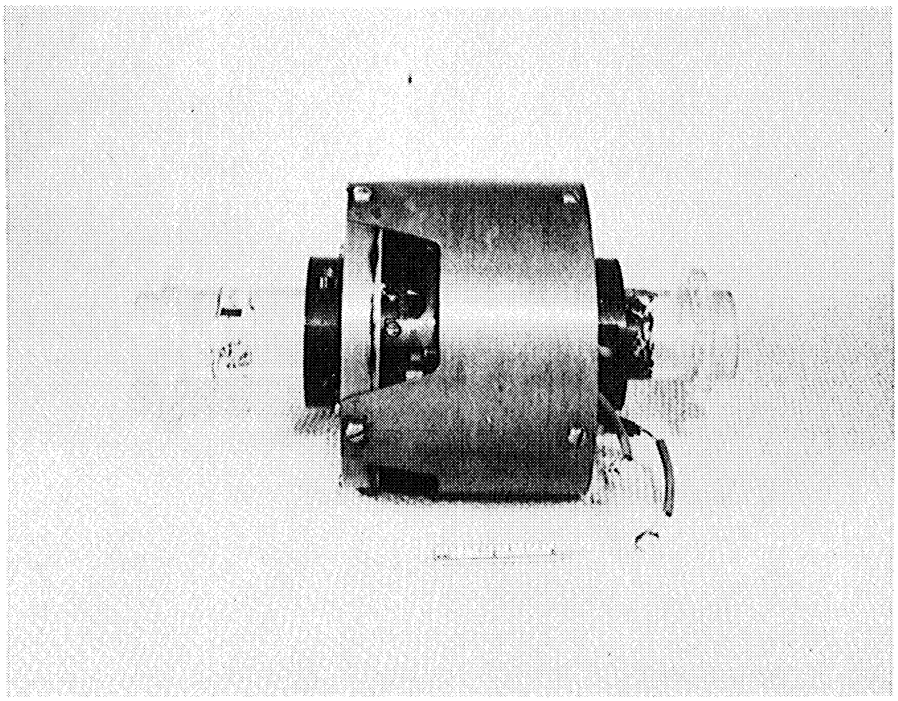

Fig. 11. Photograph of disturbance generator.

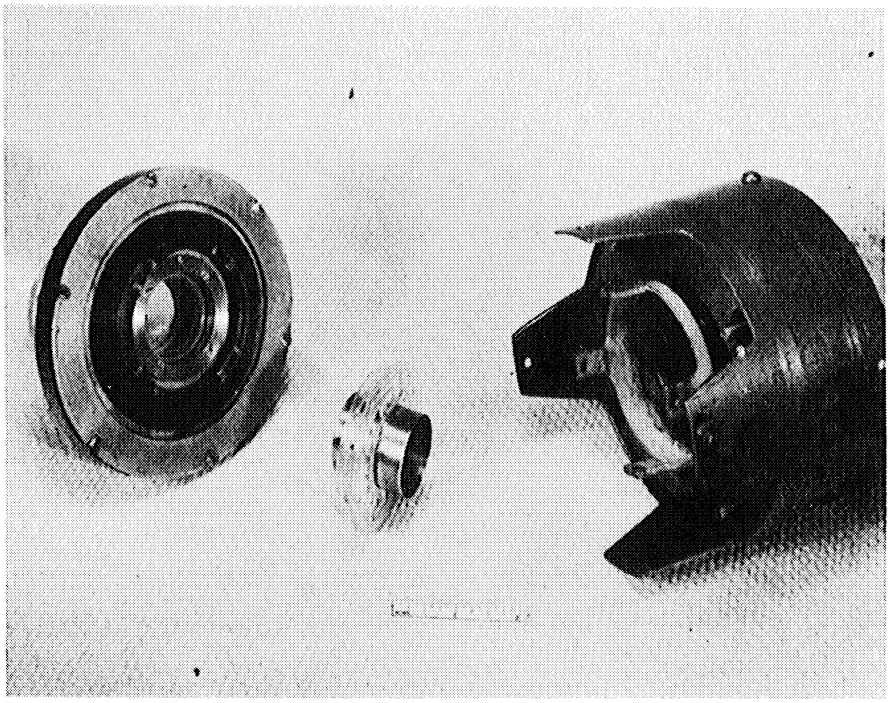

Fig. 12. Photograph of disturbance generator (exploded).

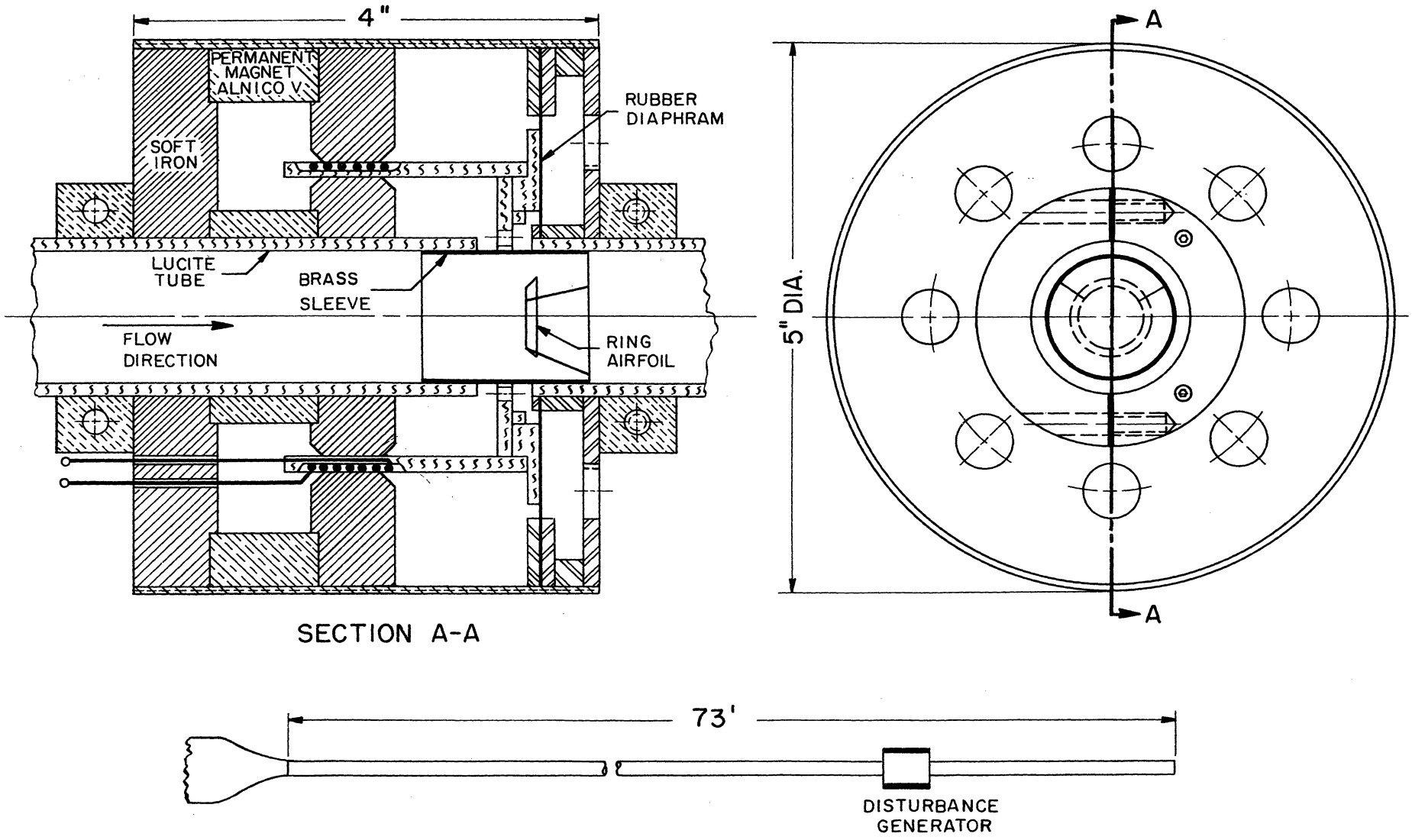

Fig. 13. Schematic diagram of disturbance generator.

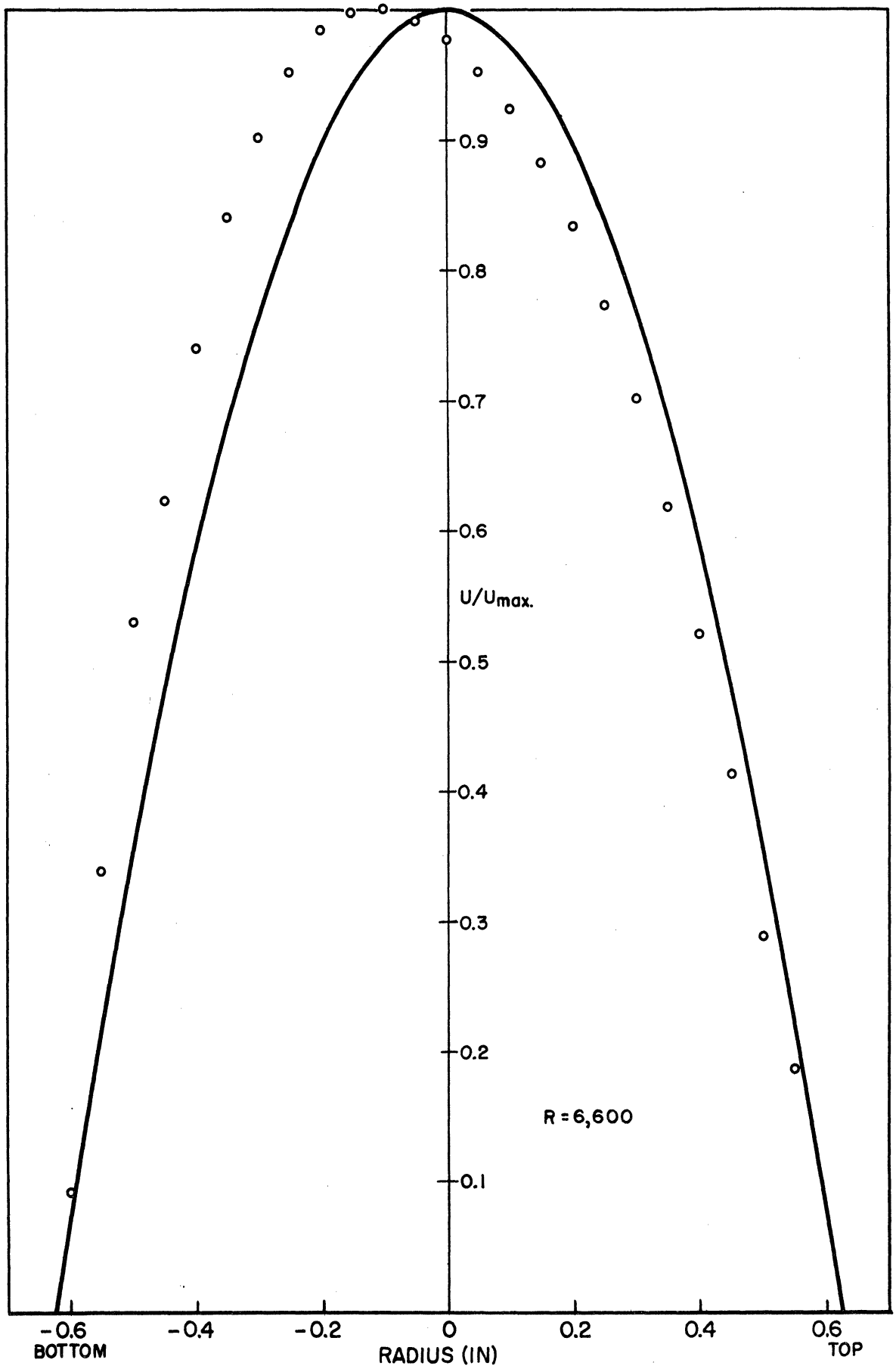

Fig. 14. Mean velocity profile (no heat added).

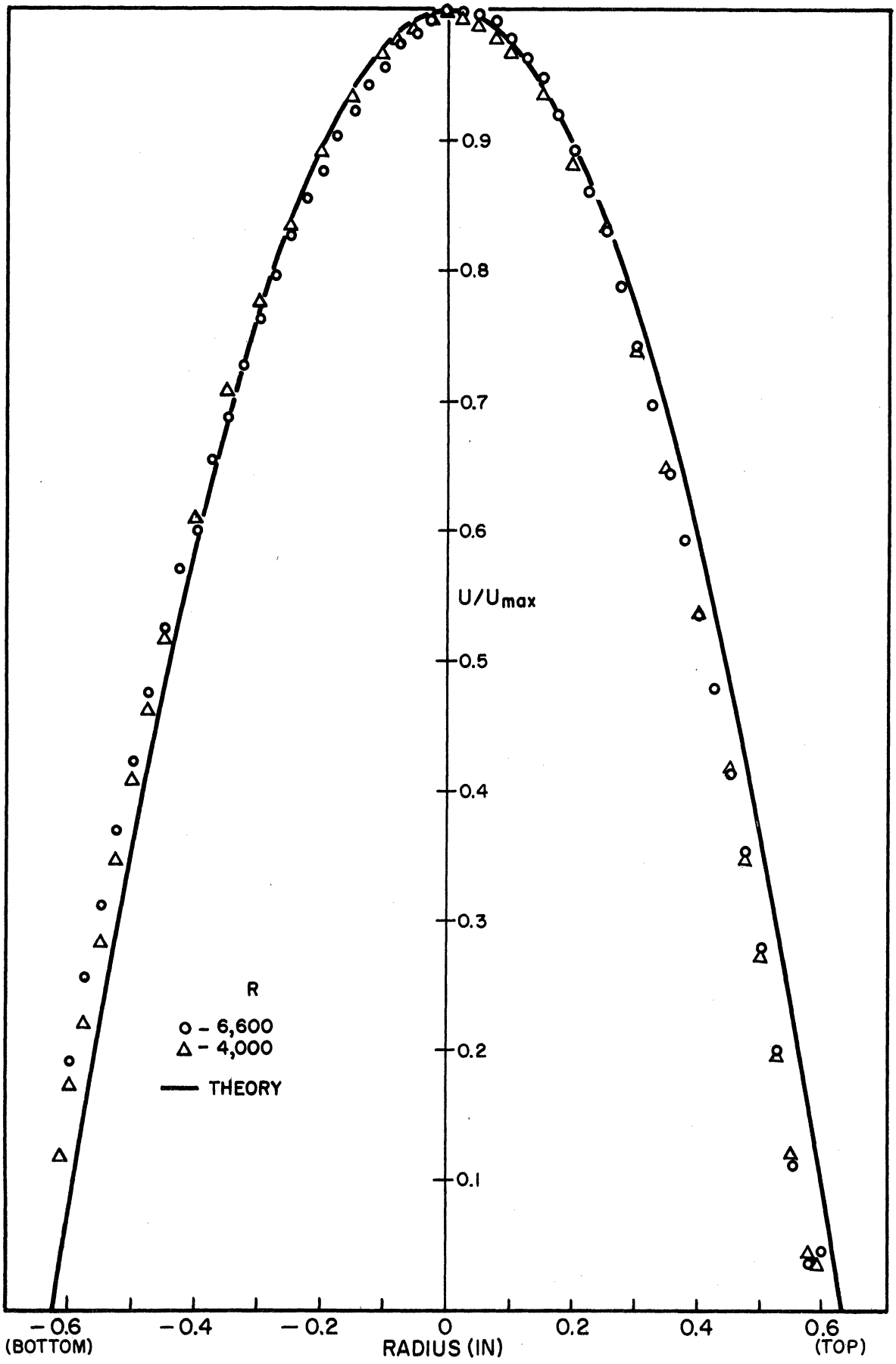

Fig. 15. Mean velocity profiles (heat added).

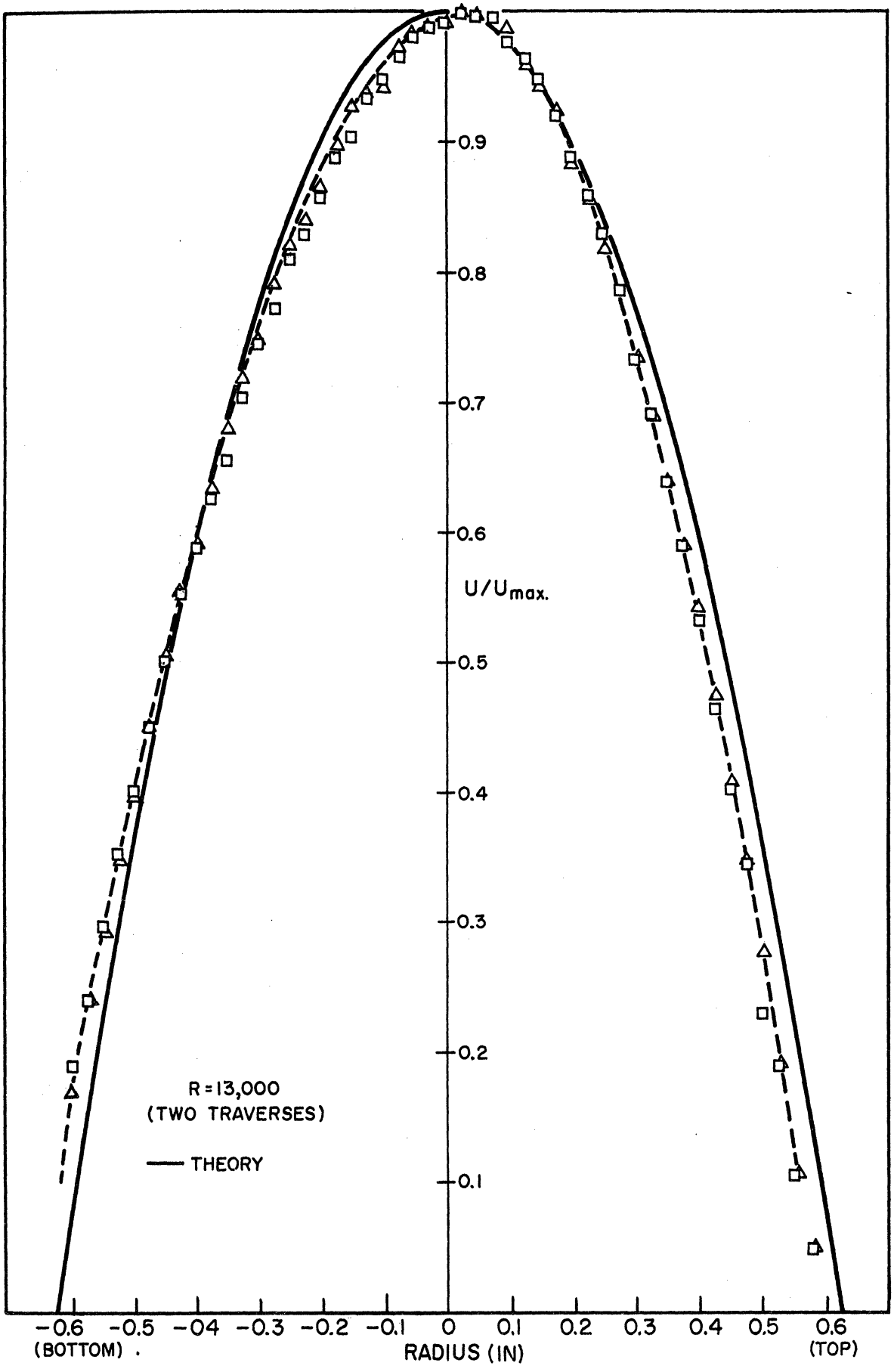

Fig. 16. Mean velocity profile (heat added).

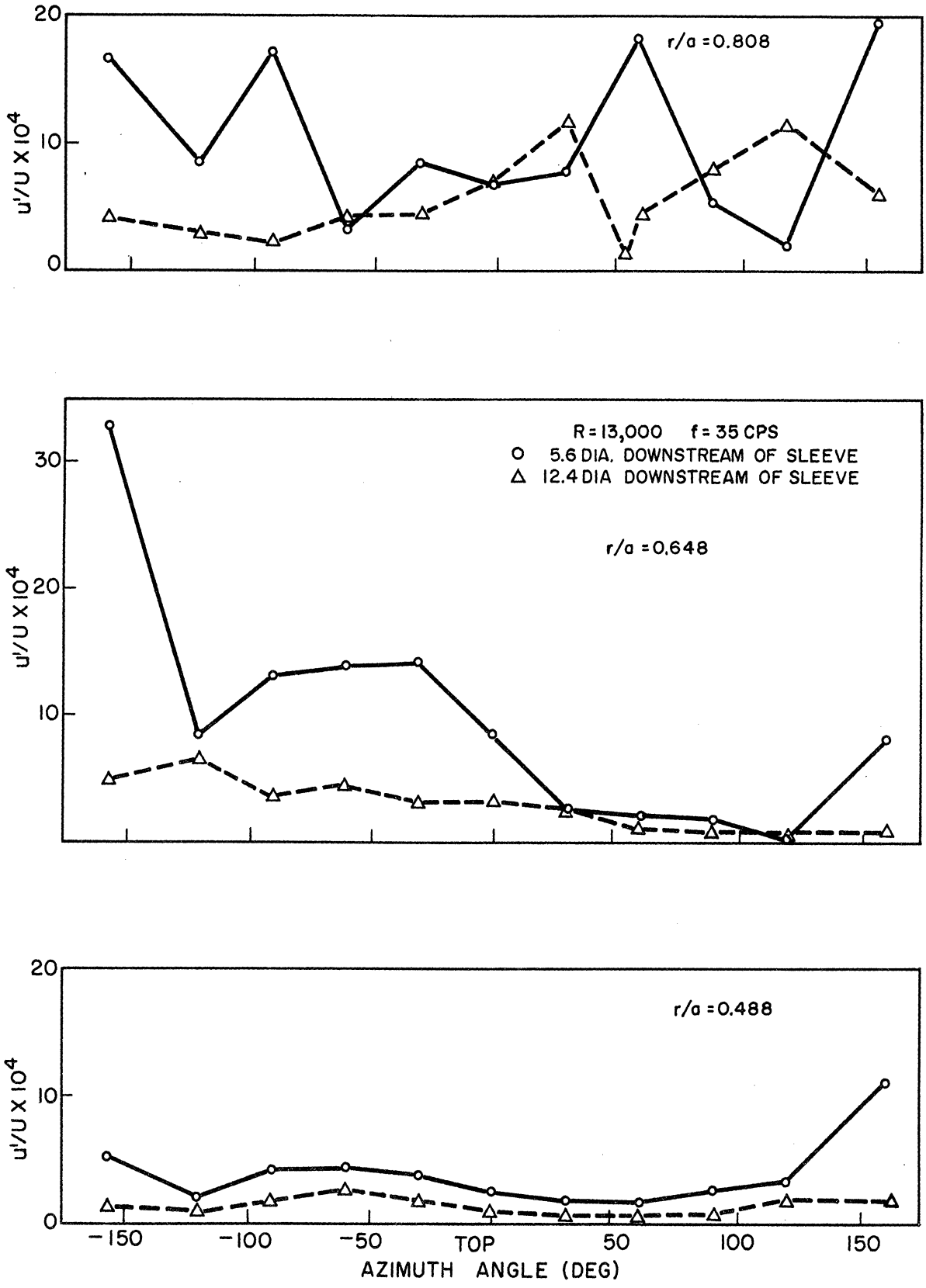

Fig. 17. Peripheral distributions of amplitude of disturbances.

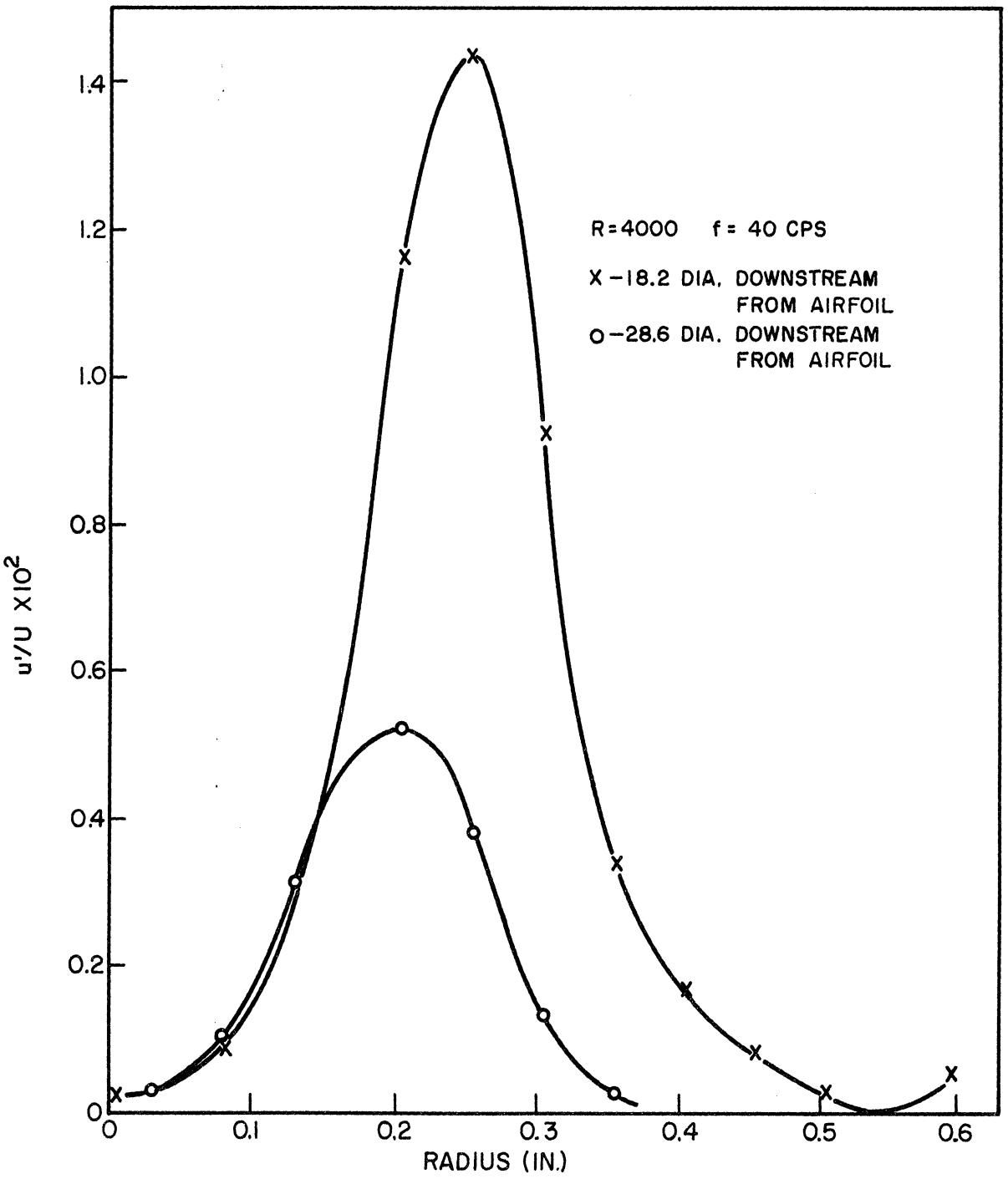

Fig. 18. Radial distributions of amplitude of disturbances.

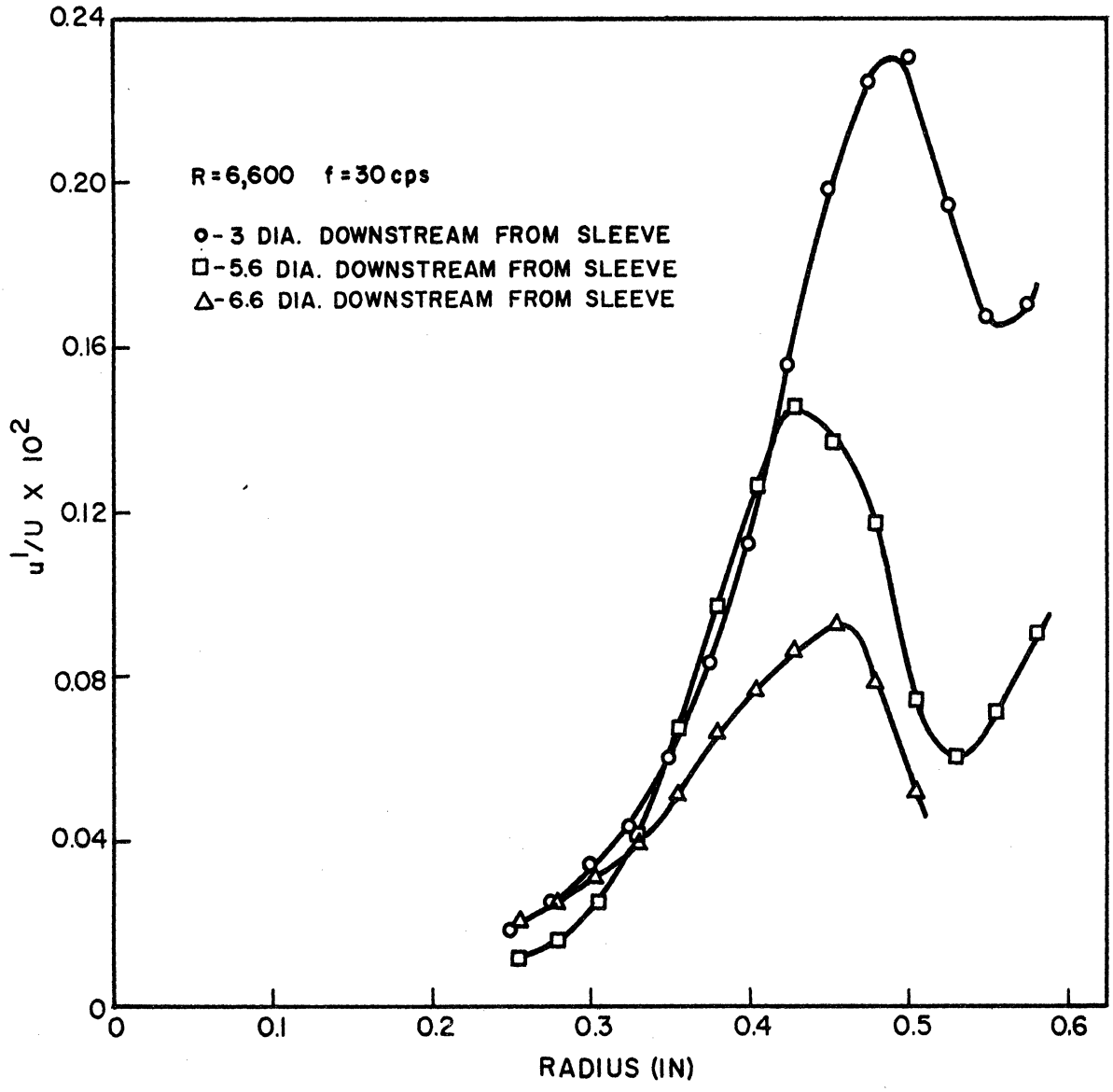

Fig. 19. Radial distributions of amplitude of disturbances.

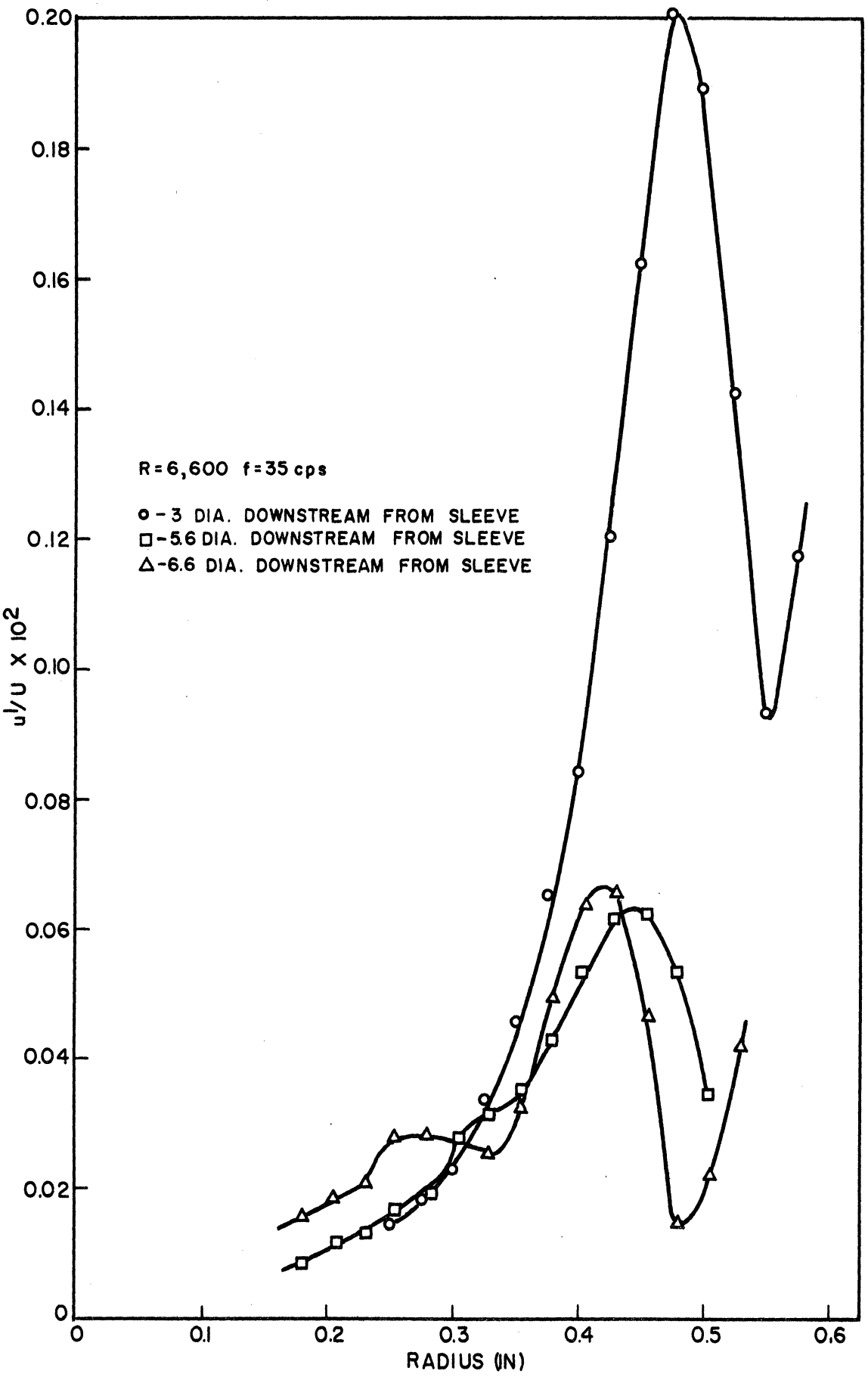

Fig. 20. Radial distributions of amplitude of disturbances.

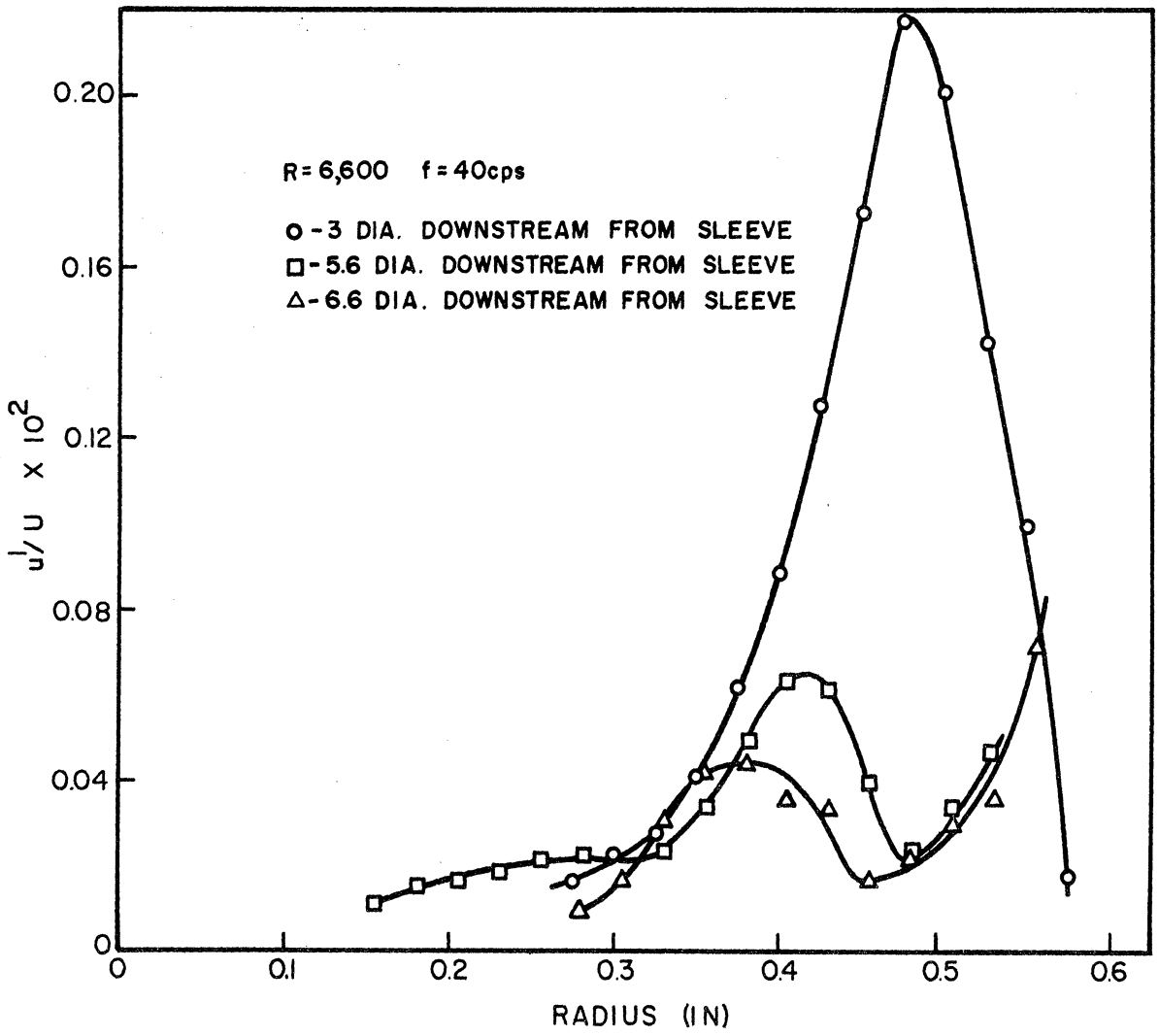

Fig. 21. Radial distributions of amplitude of disturbances.

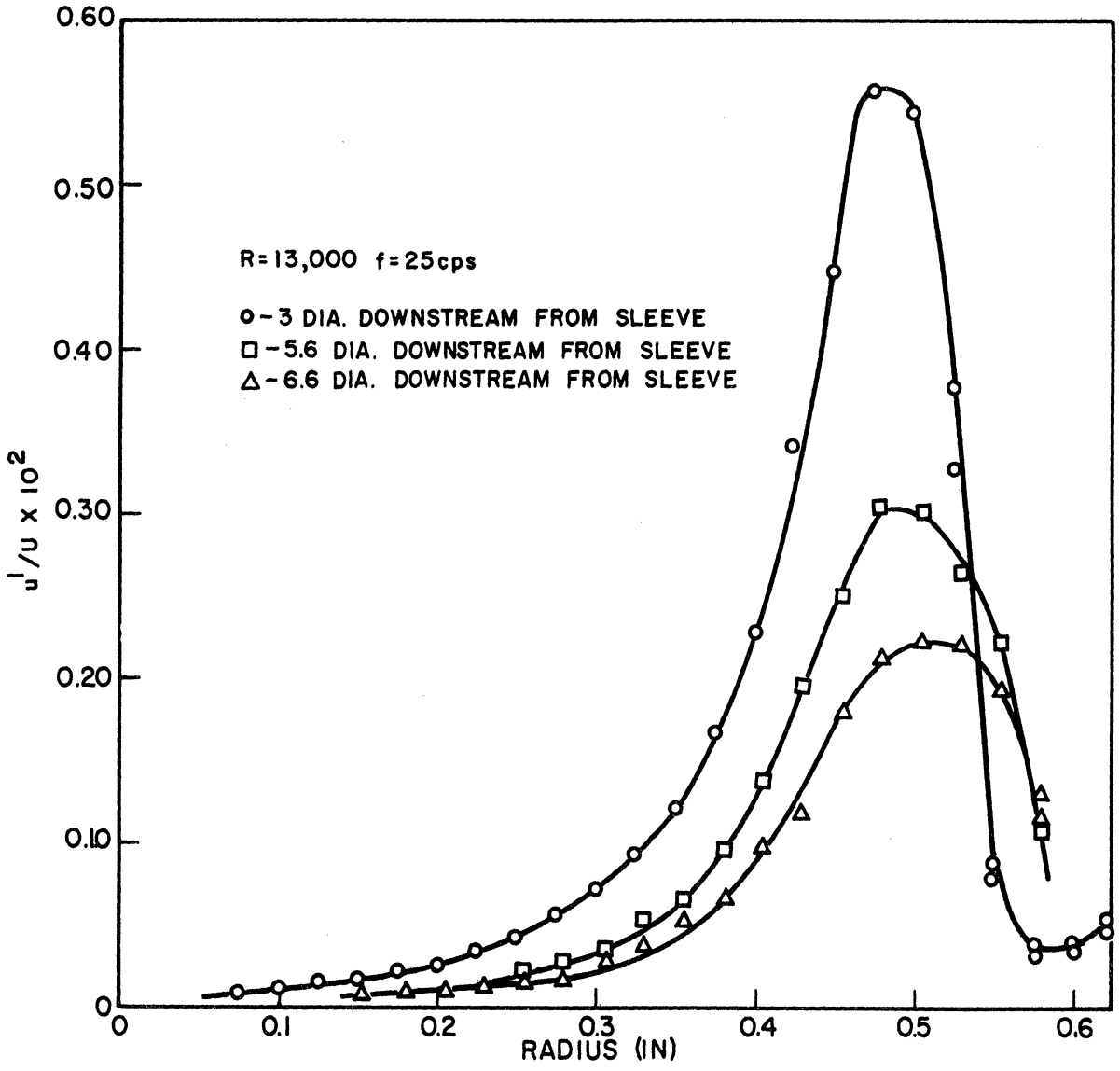

Fig. 22. Radial distributions of amplitude of disturbances.

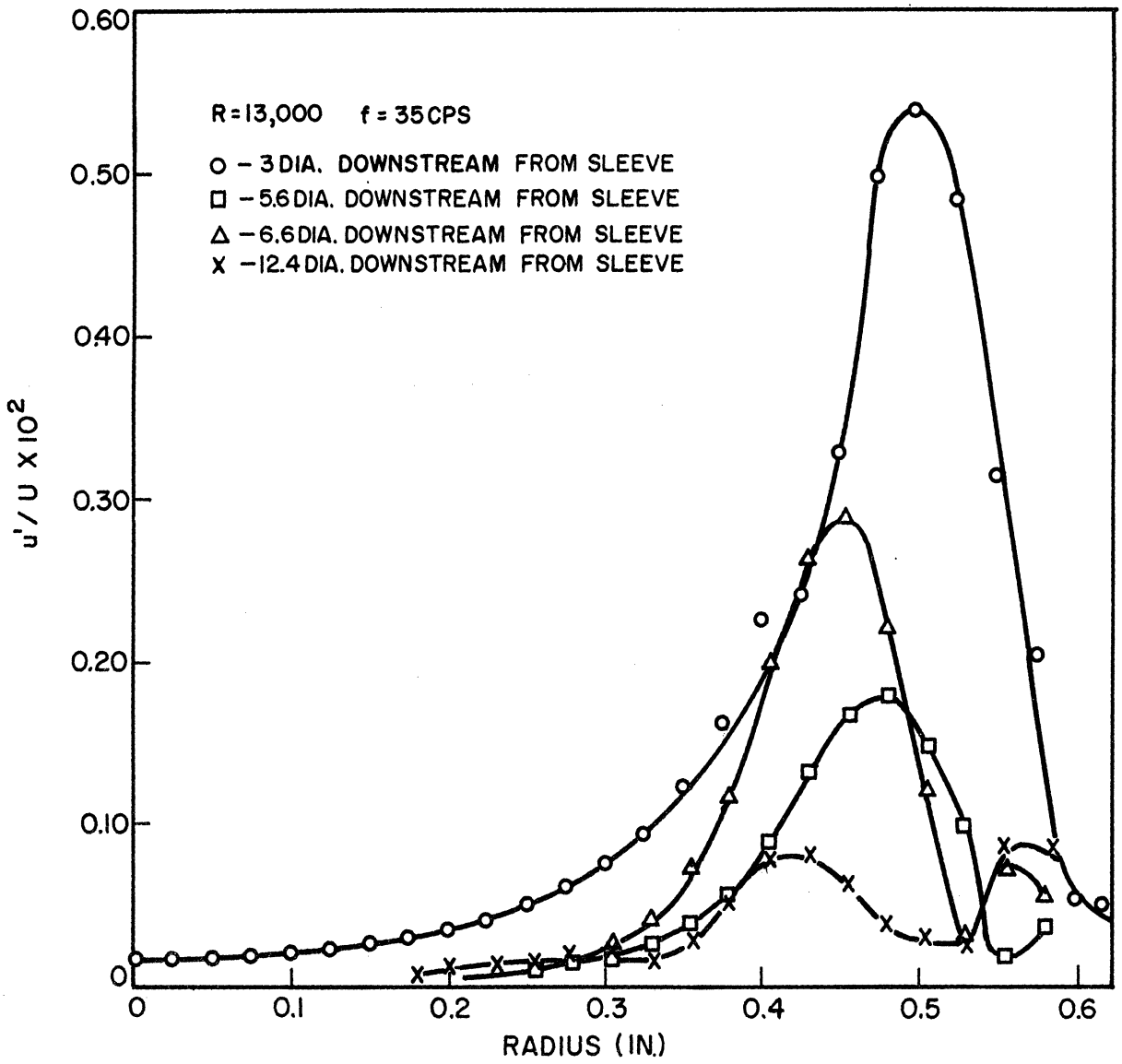

Fig. 23. Radial distributions of amplitude of disturbances.

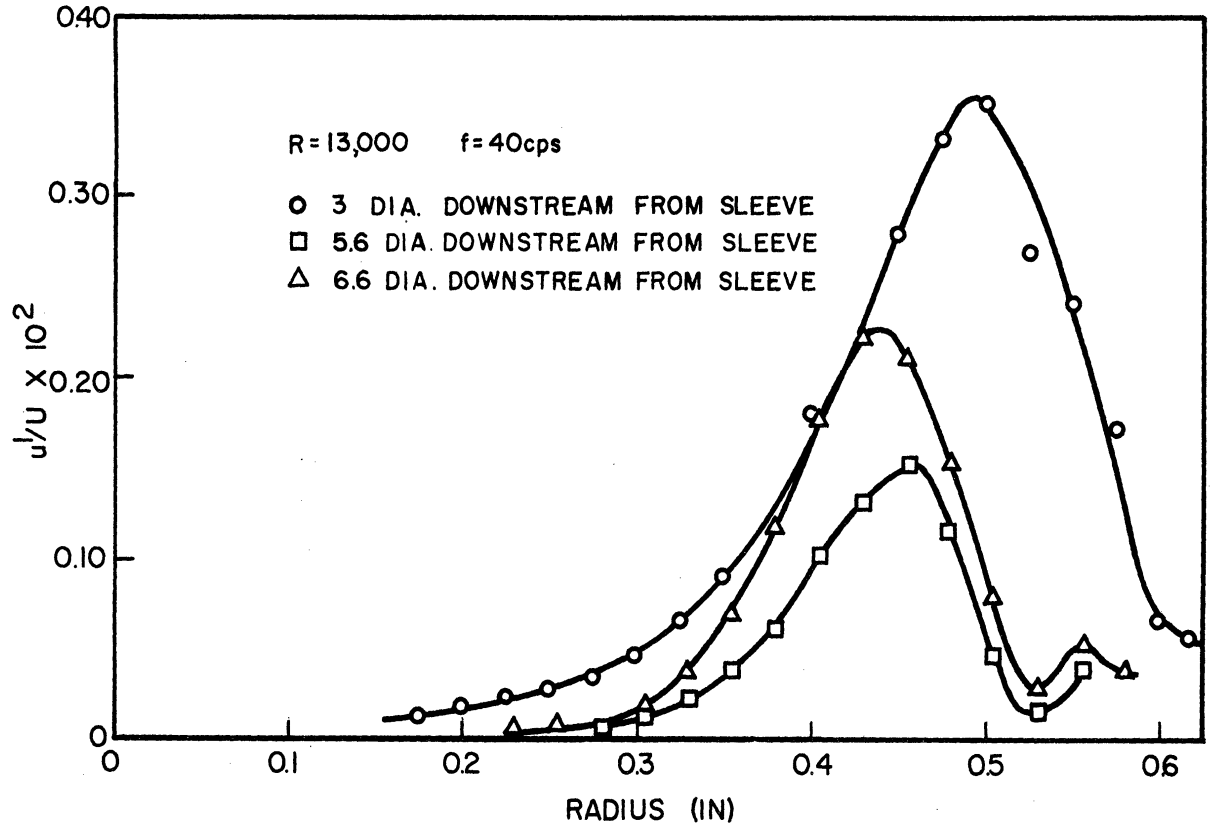

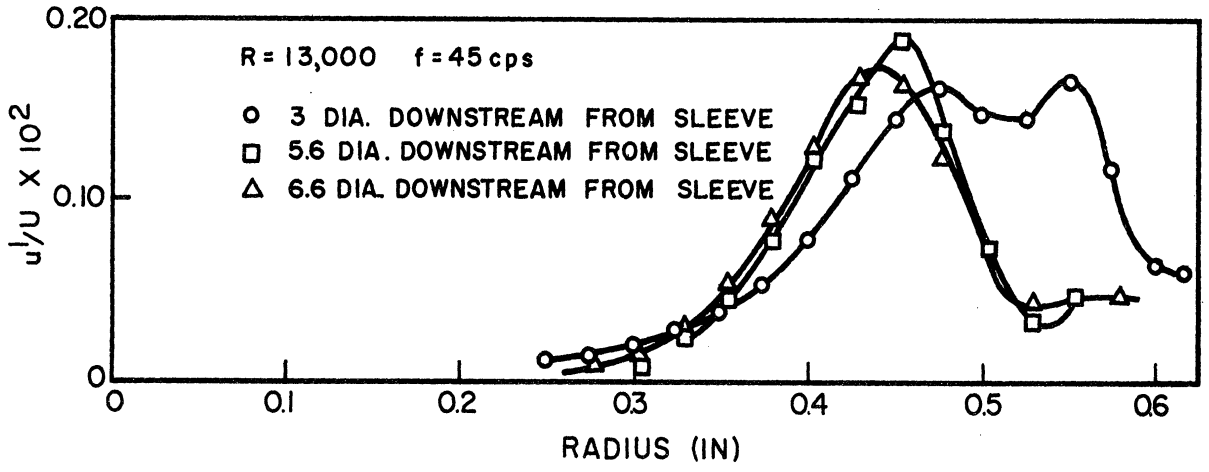

Fig. 24. Radial distributions of amplitude of disturbances.

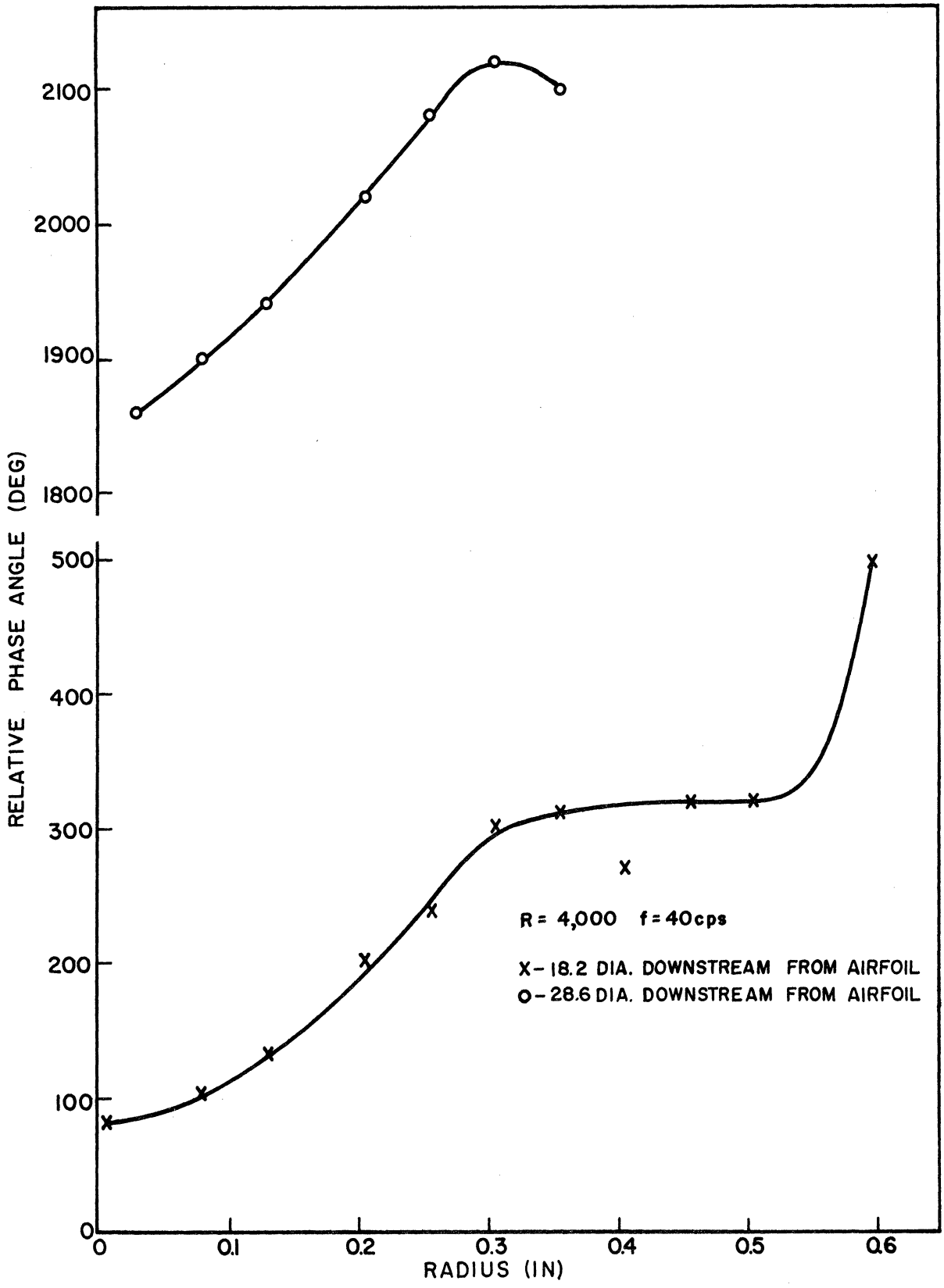

Fig. 25. Radial distributions of phase angles of disturbances.

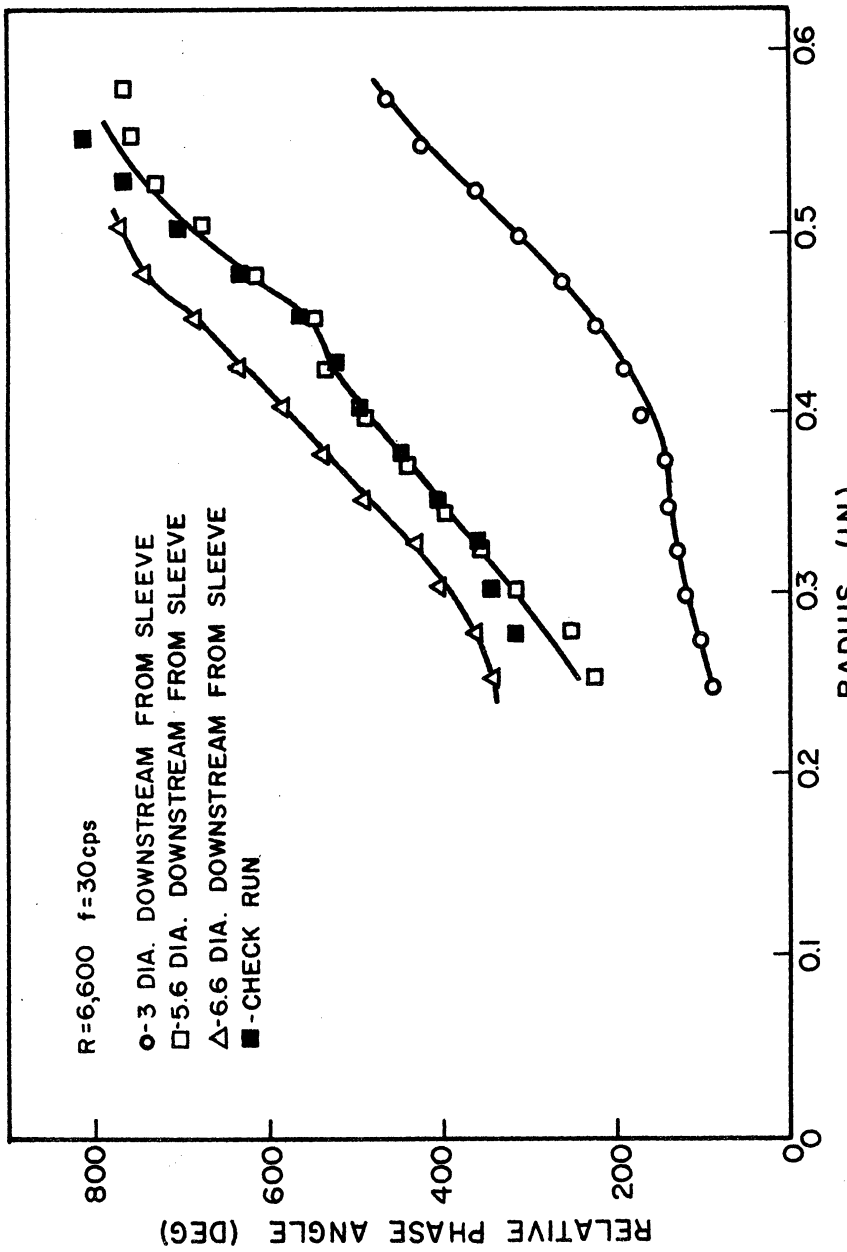

Fig. 26. Radial distributions of phase angles of disturbances.

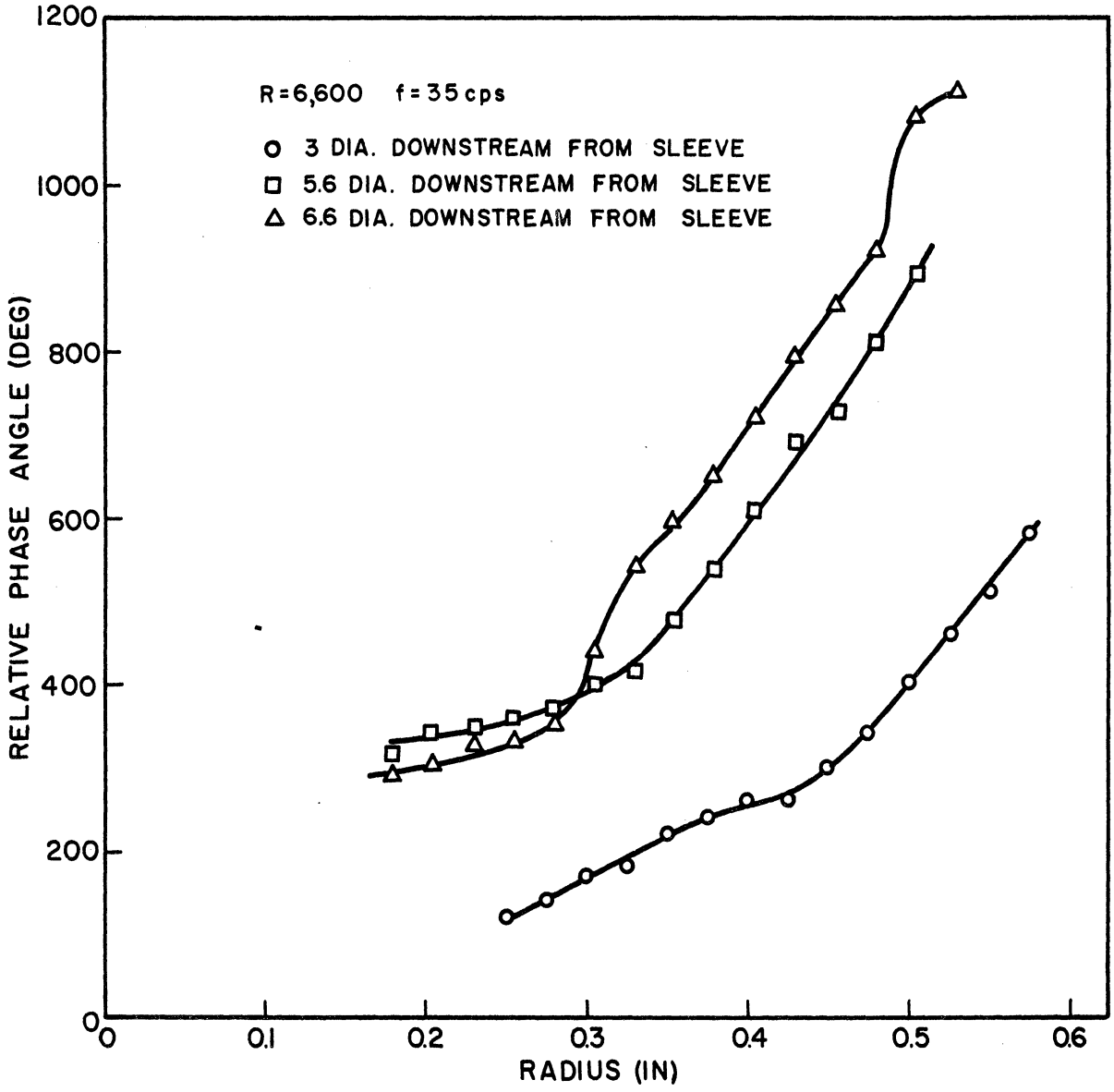

Fig. 27. Radial distributions of phase angles of disturbances.

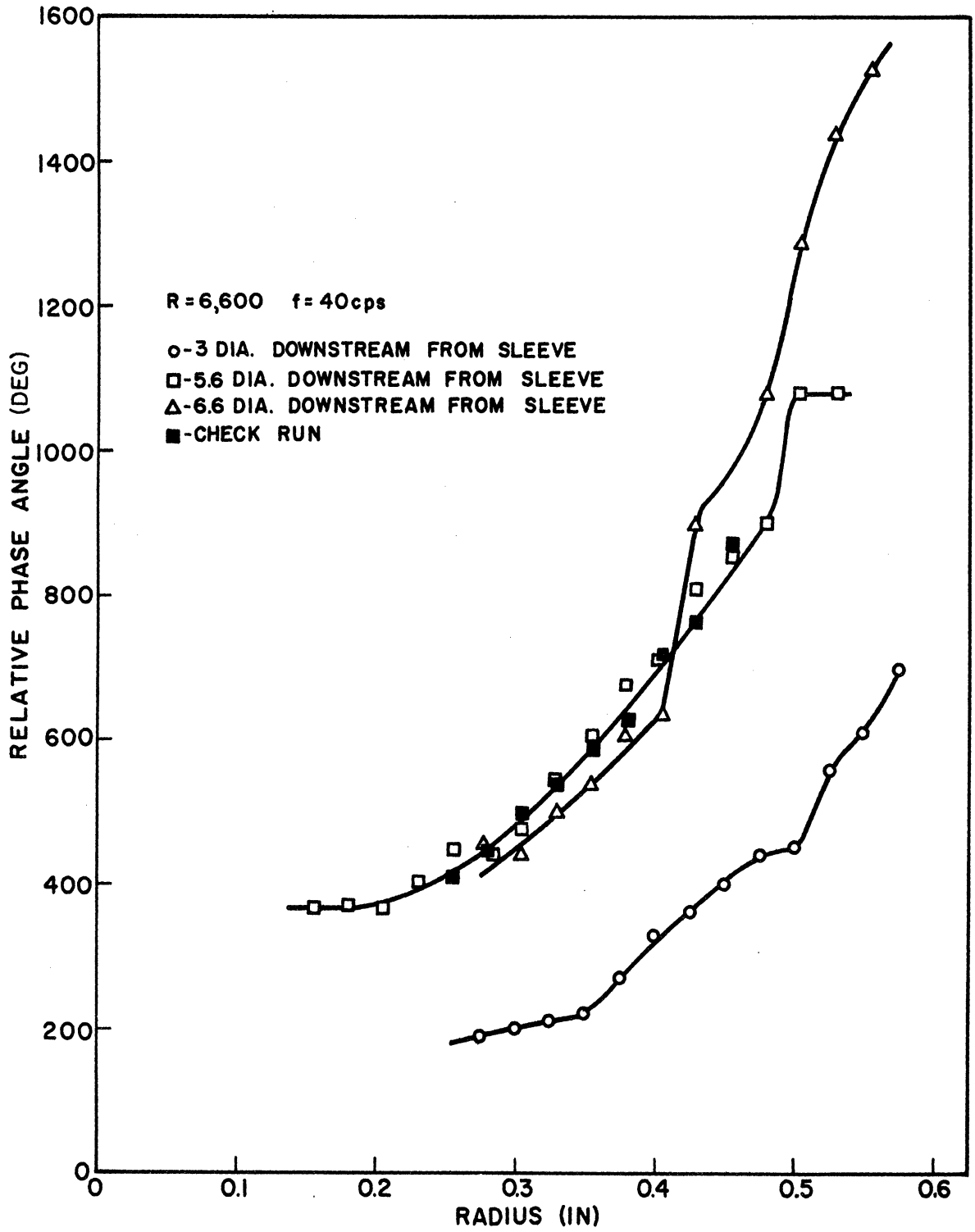

Fig. 28. Radial distributions of phase angles of disturbances.

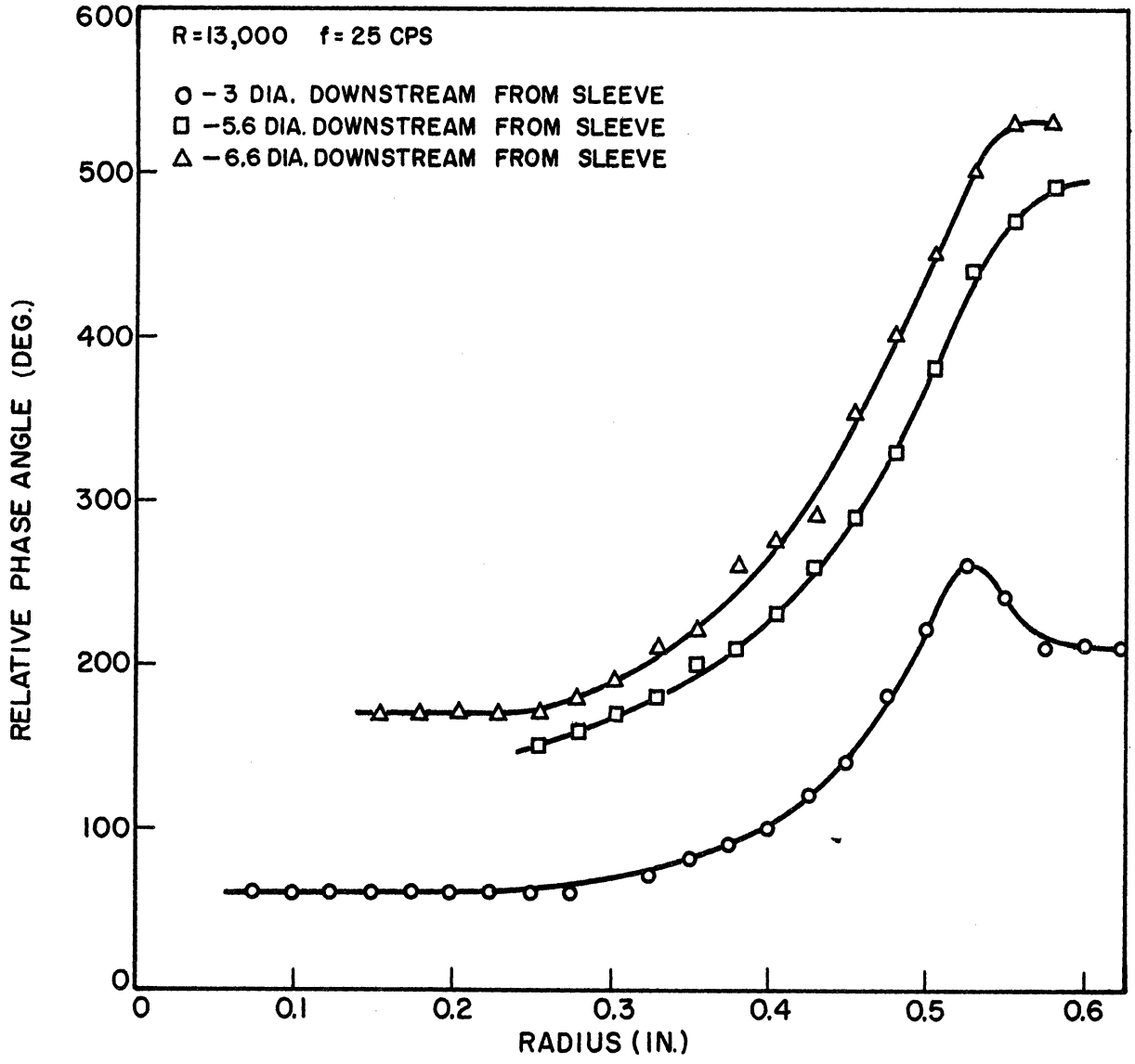

Fig. 29. Radial distributions of phase angles of disturbances.

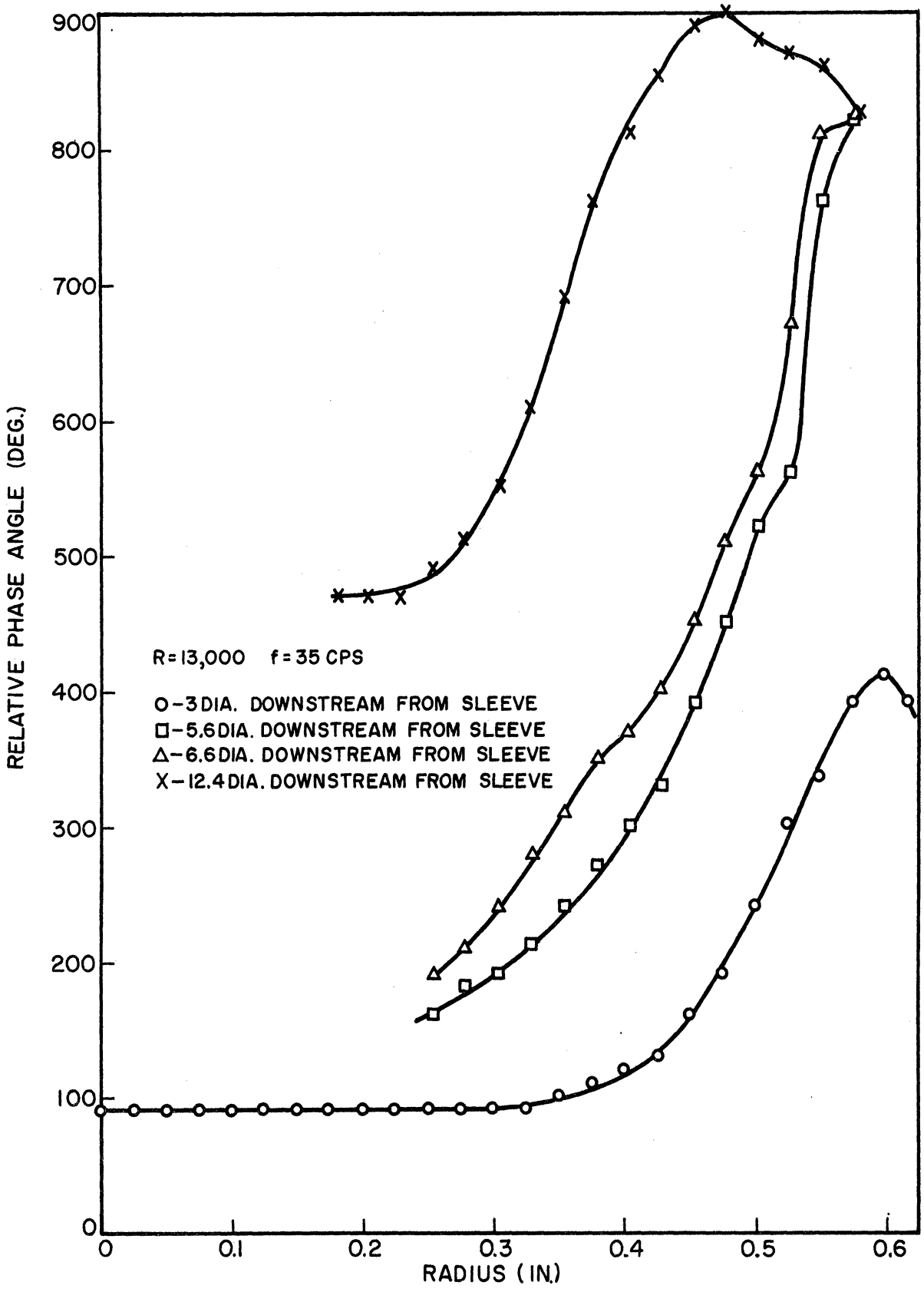

Fig. 30. Radial distributions of phase angles of disturbances.

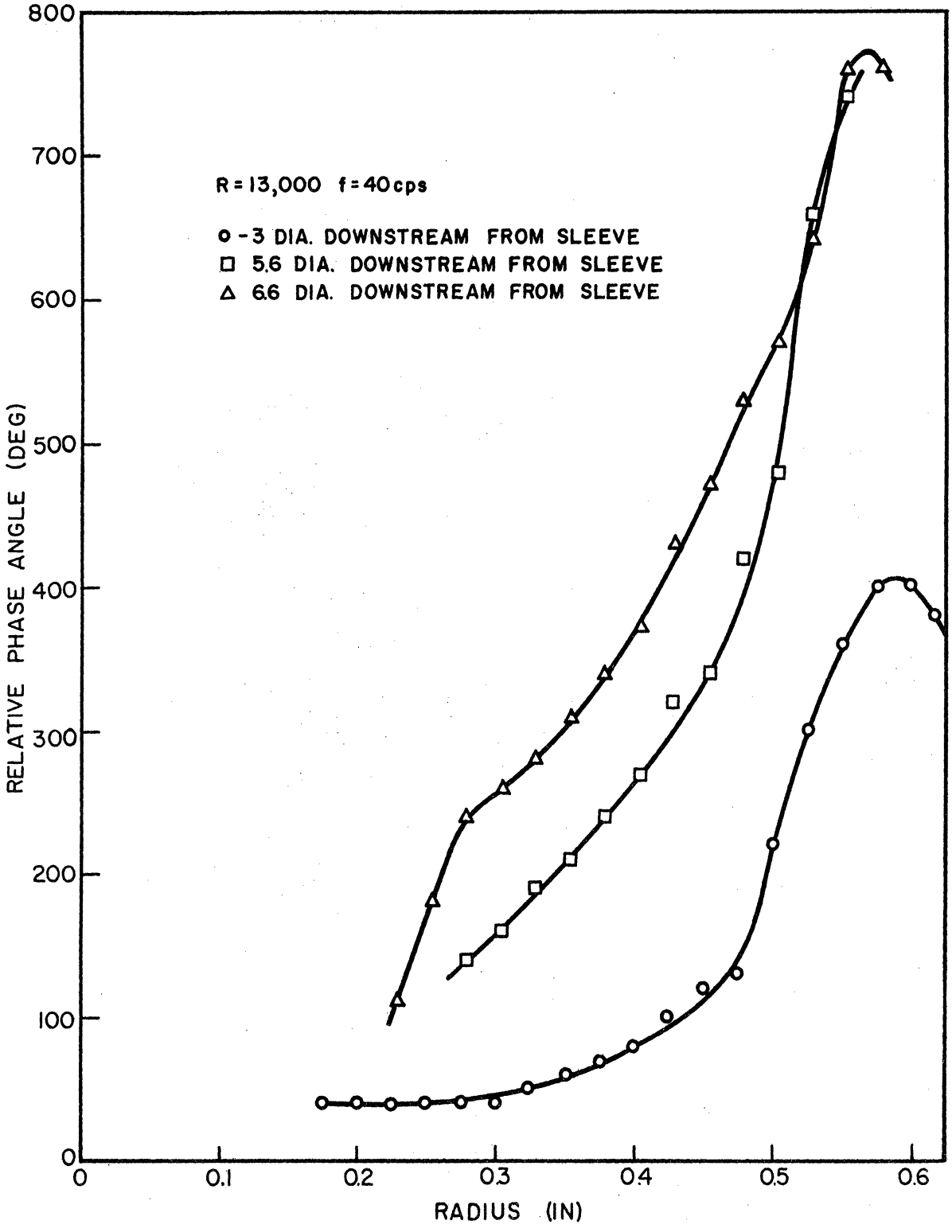

Fig. 31. Radial distributions of phase angles of disturbances.

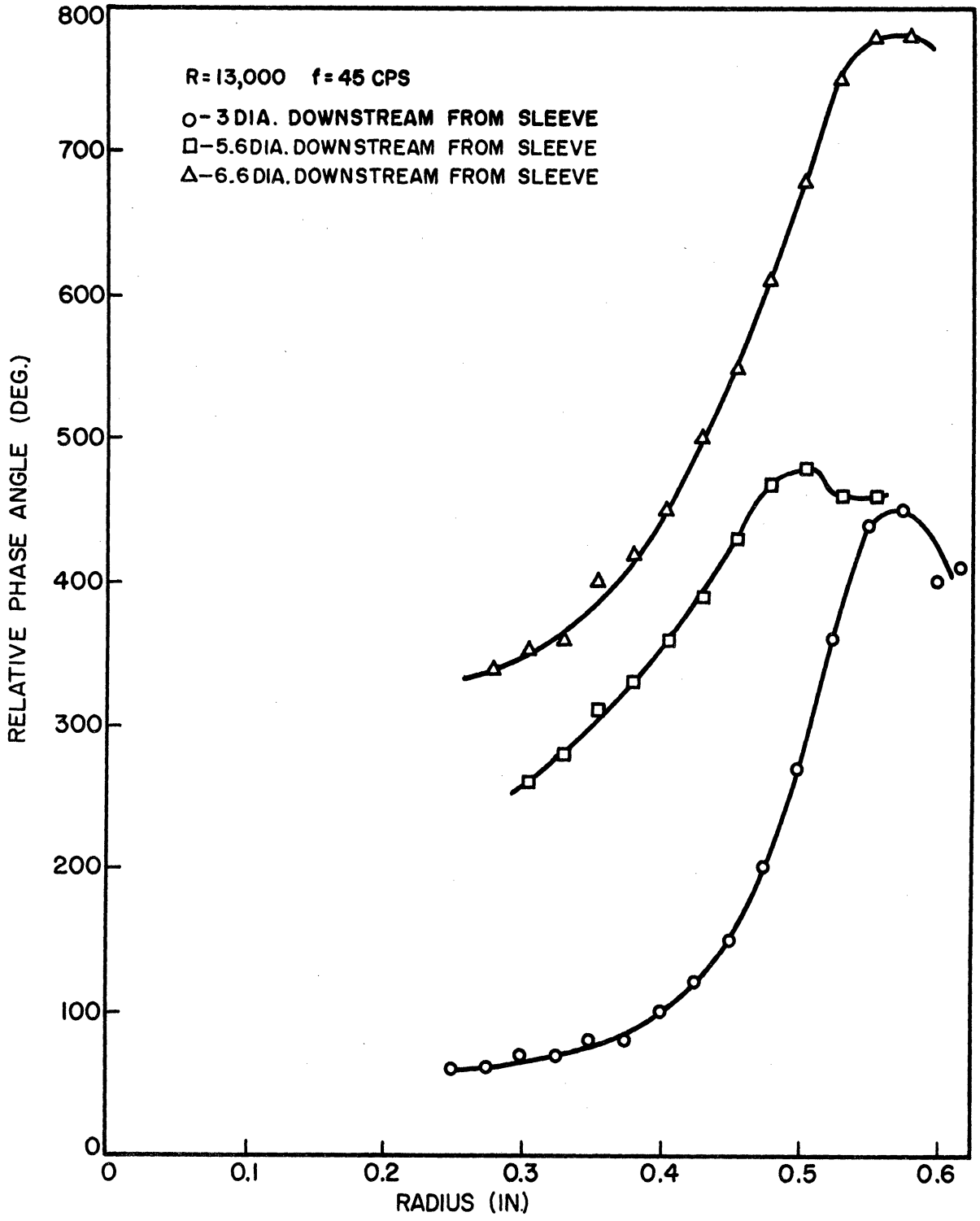

Fig. 32. Radial distributions of phase angles of disturbances.

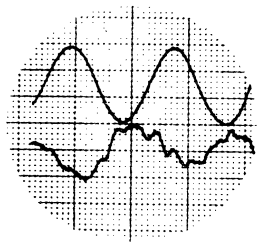

1. r/a = 0.952; θ = 600°
u'/U = 1.20 x 10^{-3}

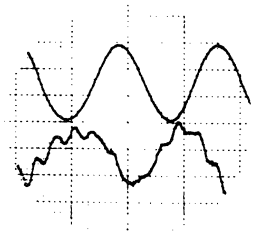

2. r/a = 0.928; θ = 590°
u'/U = 1.20 x 10^{-3}

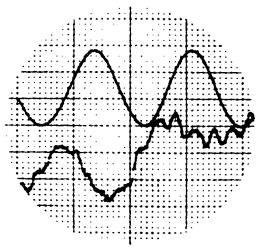

3. r/a = 0.888; θ = 590°
u'/U = 0.52 x 10^{-3}

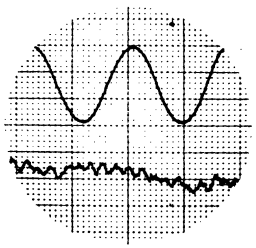

4. r/a = 0.792; θ --
u'/U = 0

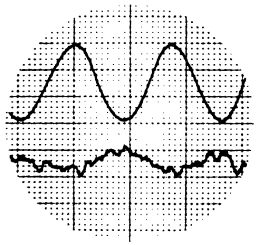

5. r/a = 0.688; θ = 540°
u'/U = 0.23 x 10^{-3}

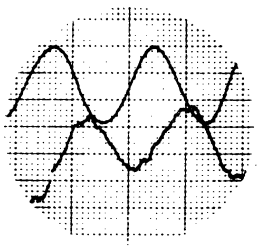

6. r/a = 0.648; θ = 490°
u'/U = 0.48 x 10^{-3}

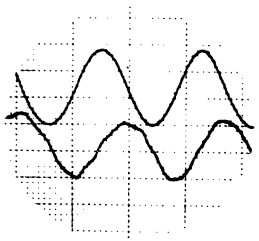

7. r/a = 0.608; θ = 460°
u'/U = 0.89 x 10^{-3}

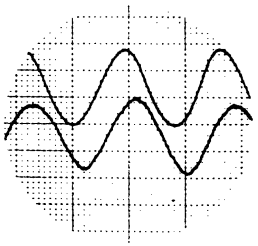

8. r/a = 0.568; θ = 420°
u'/U = 1.15 x 10^{-3}

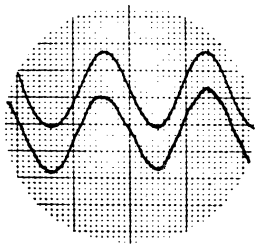

9. r/a = 0.488; θ = 360°
u'/U = 1.32 x 10^{-3}

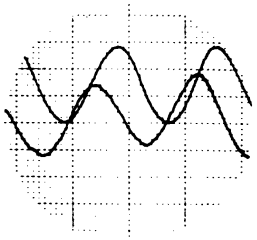

10. r/a = 0.408; θ = 300°
u'/U = 1.05 x 10^{-3}

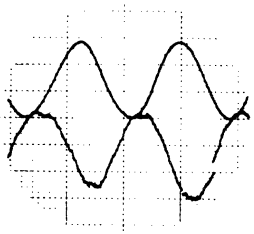

11. r/a = 0.328; θ = 230°
u'/U = 0.52 x 10^{-3}

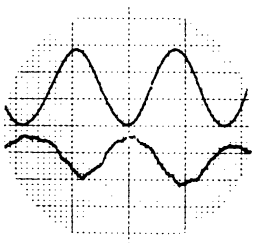

12. r/a = 0.248; θ = 190°
u'/U = 0.22 x 10^{-3}

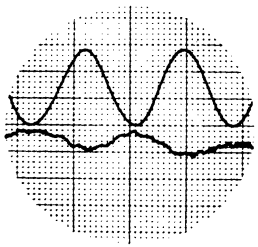

13. r/a = 0.128; θ = 180°
u'/U = 0.11 x 10^{-3}

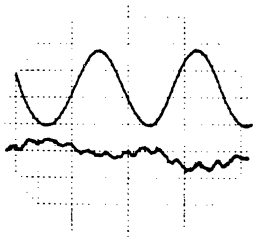

14. r/a = 0; θ = 180°
u'/U = 0.02 x 10^{-3}

R = 4,000 f = 40 cps

STATION - 18.2 dia. downstream of airfoil

Fig. 33. Radial distribution of disturbances.

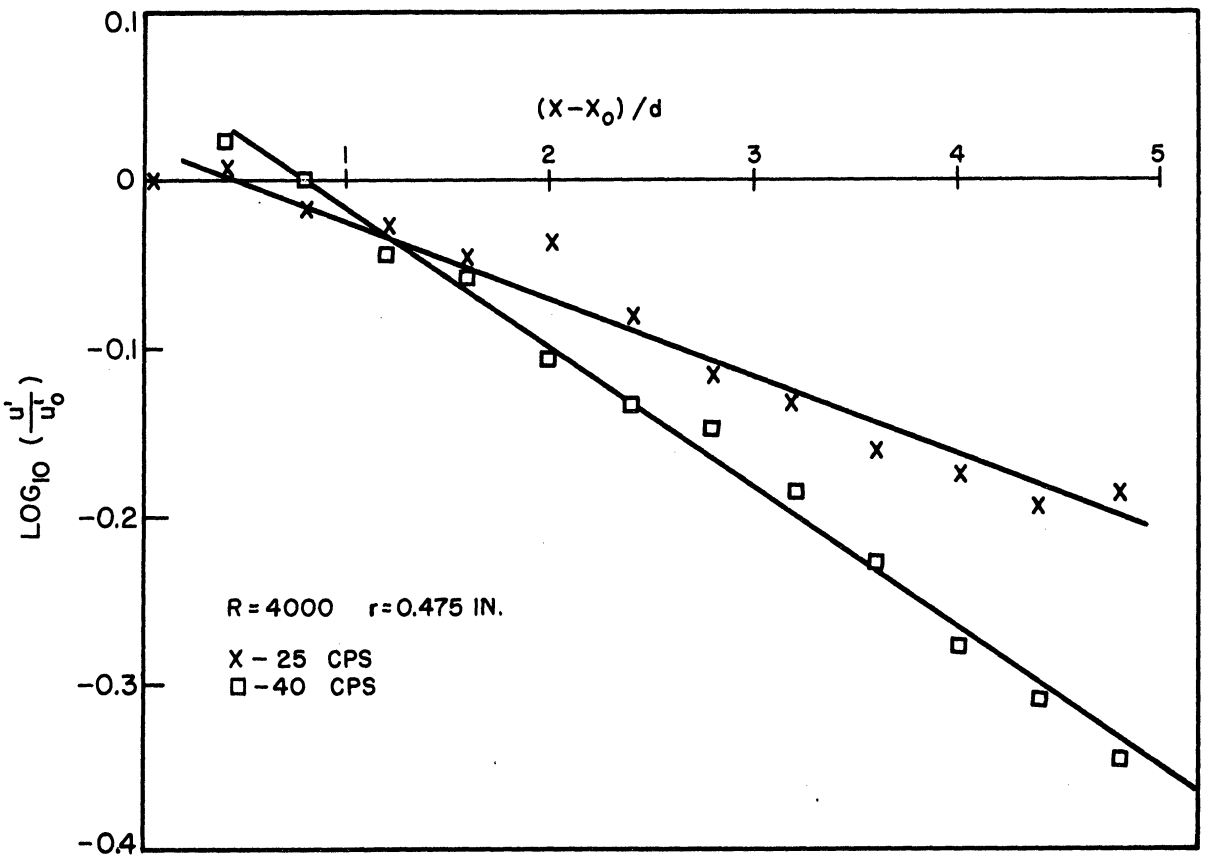

Fig. 34. Decay of u-component of disturbances.

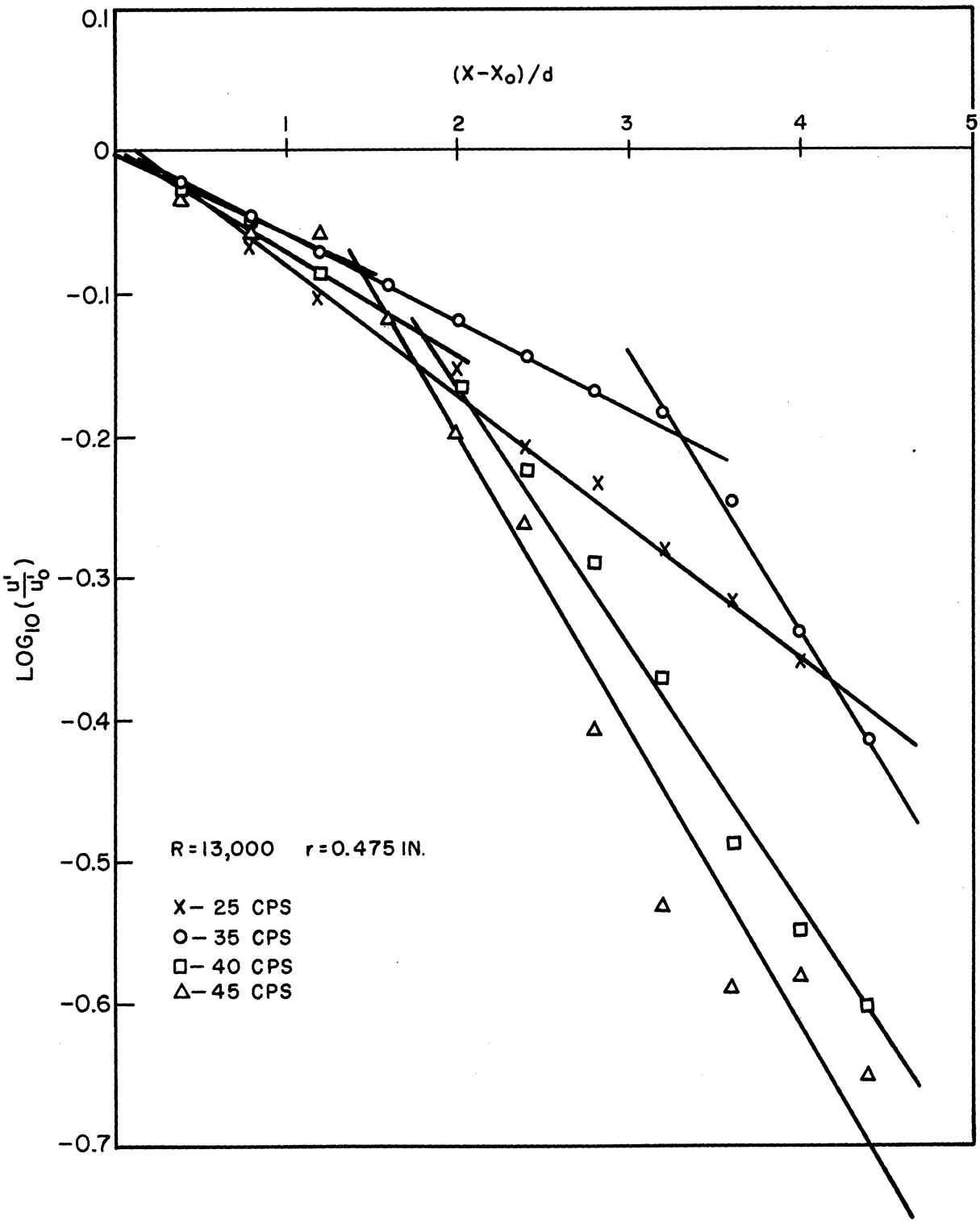

Fig. 35. Decay of u-component of disturbances.

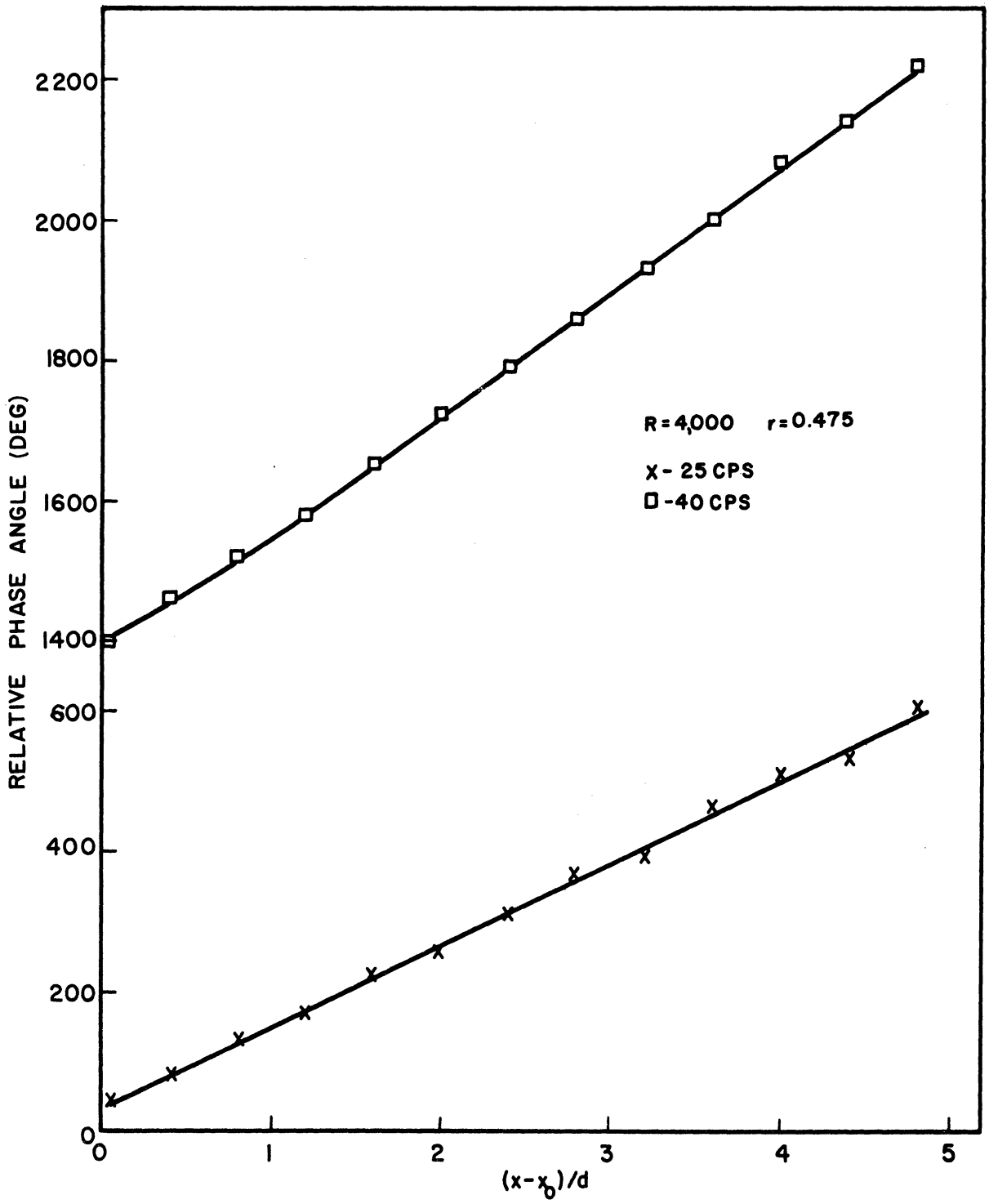

Fig. 36. Longitudinal distributions of phase angles of disturbances.

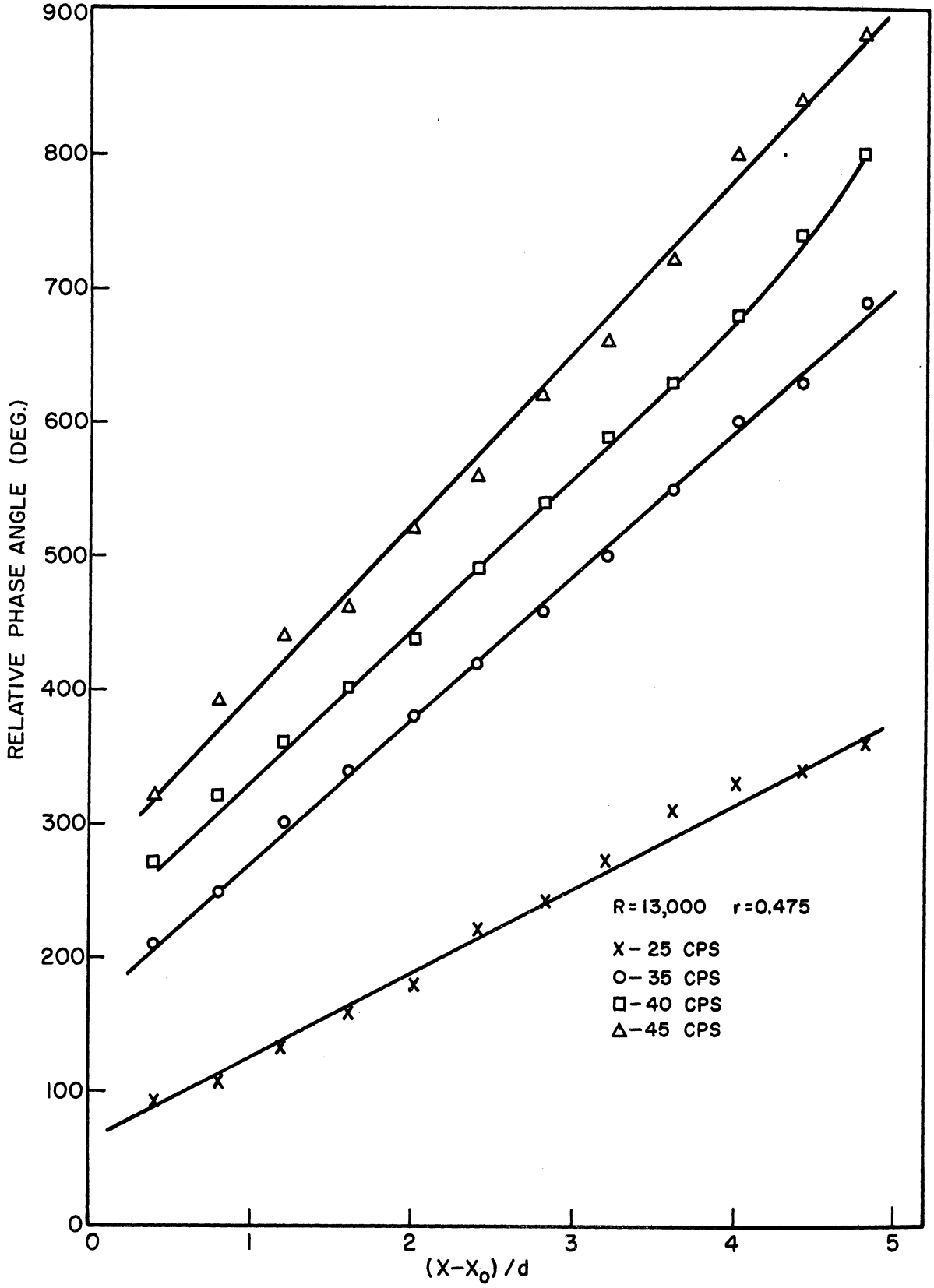

Fig. 37. Longitudinal distributions of phase angles of disturbances.

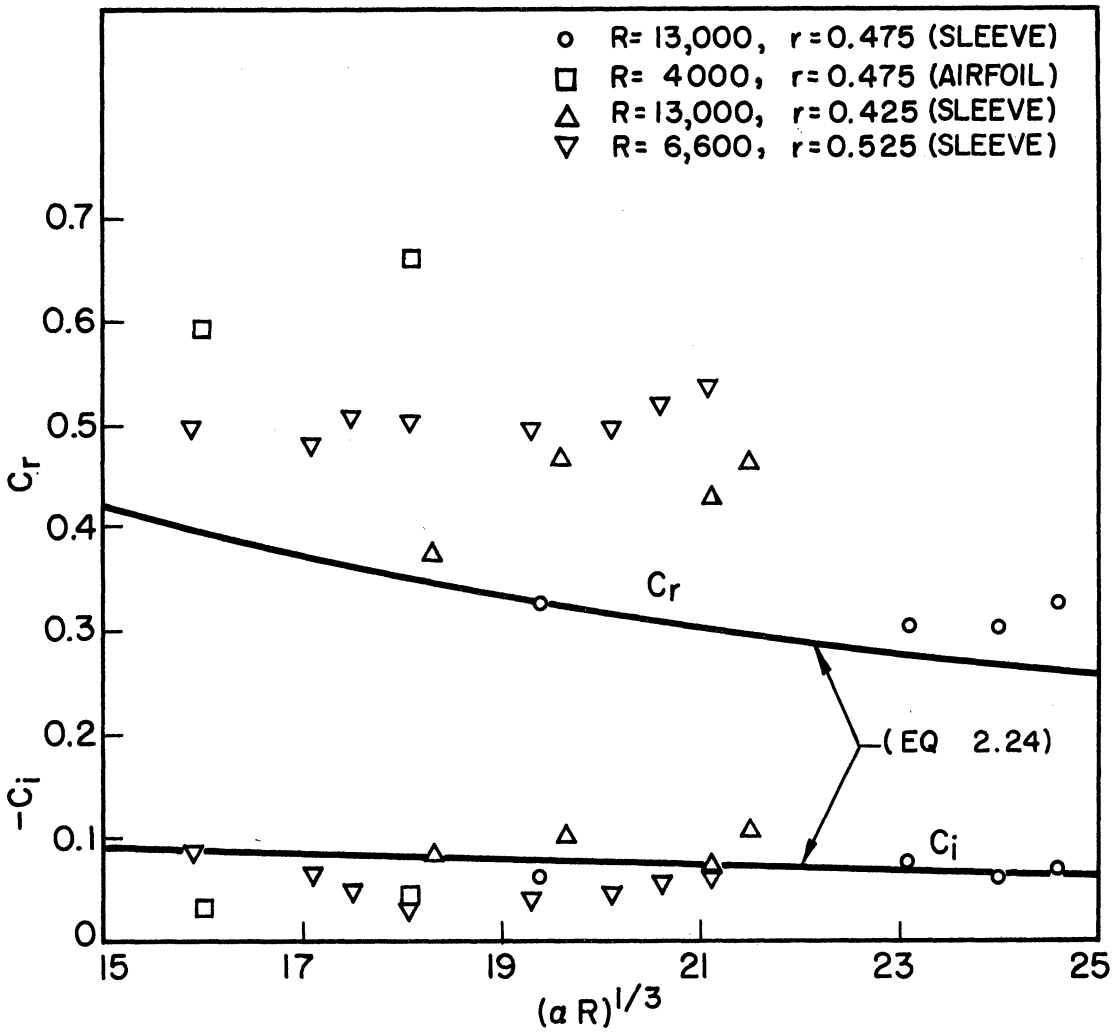

Fig. 38. c_r and - c_i vs $(\alpha R)^{1/3}$, comparison of experimental results with theoretical predictions.

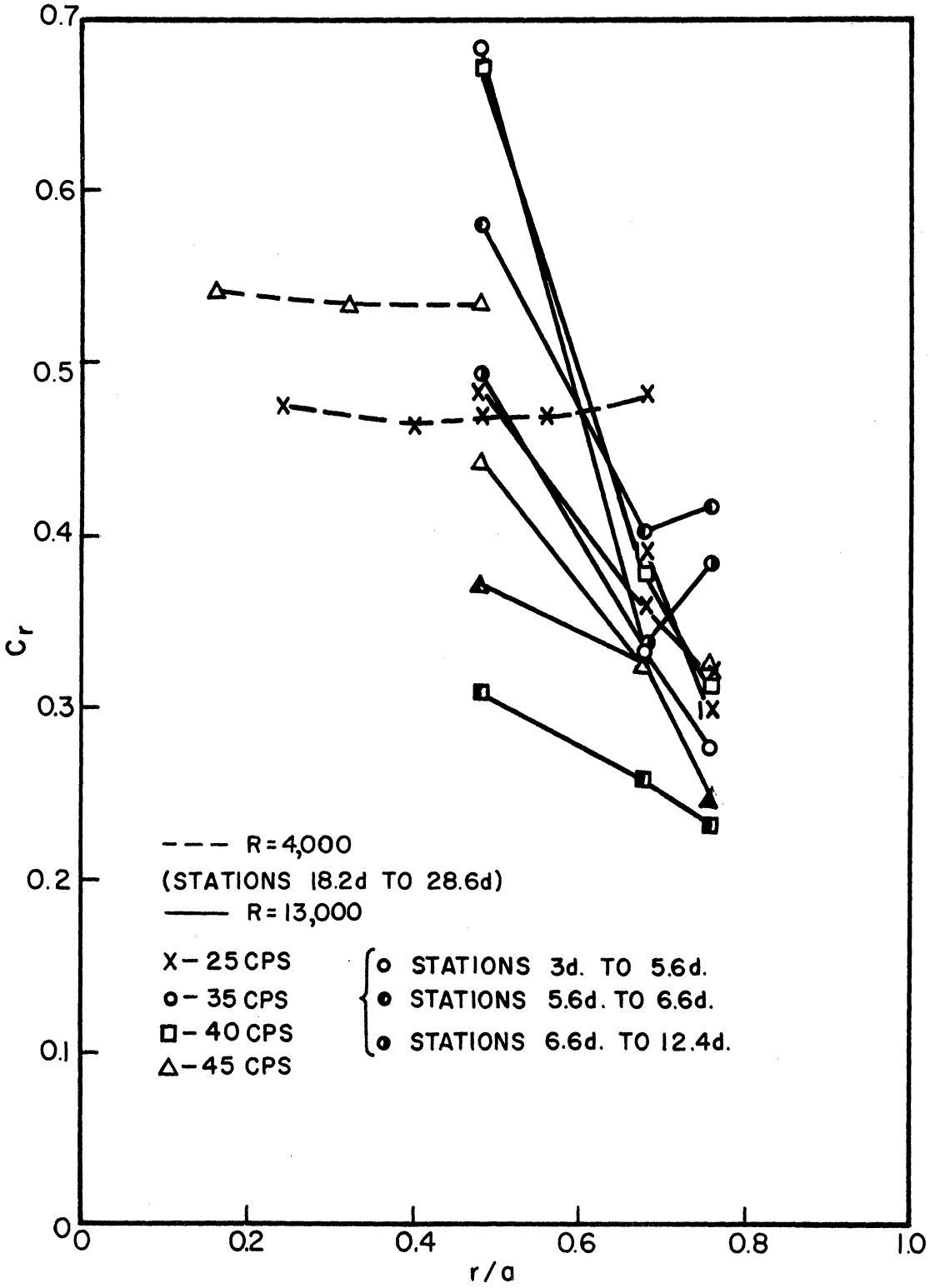

Fig. 39. Radial variation of wave propagation velocity.

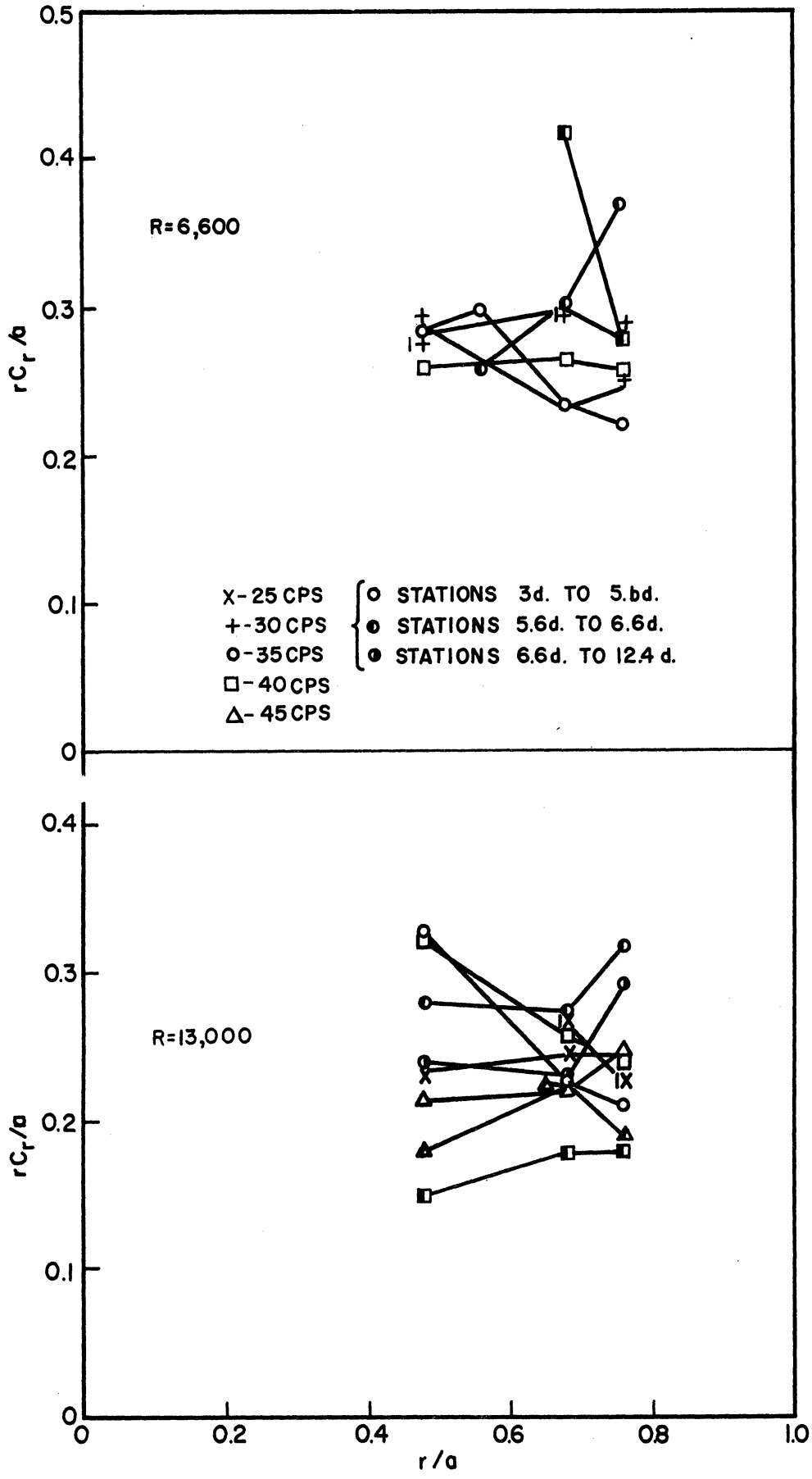

Fig. 40. Radial variation of wave propagation velocity.

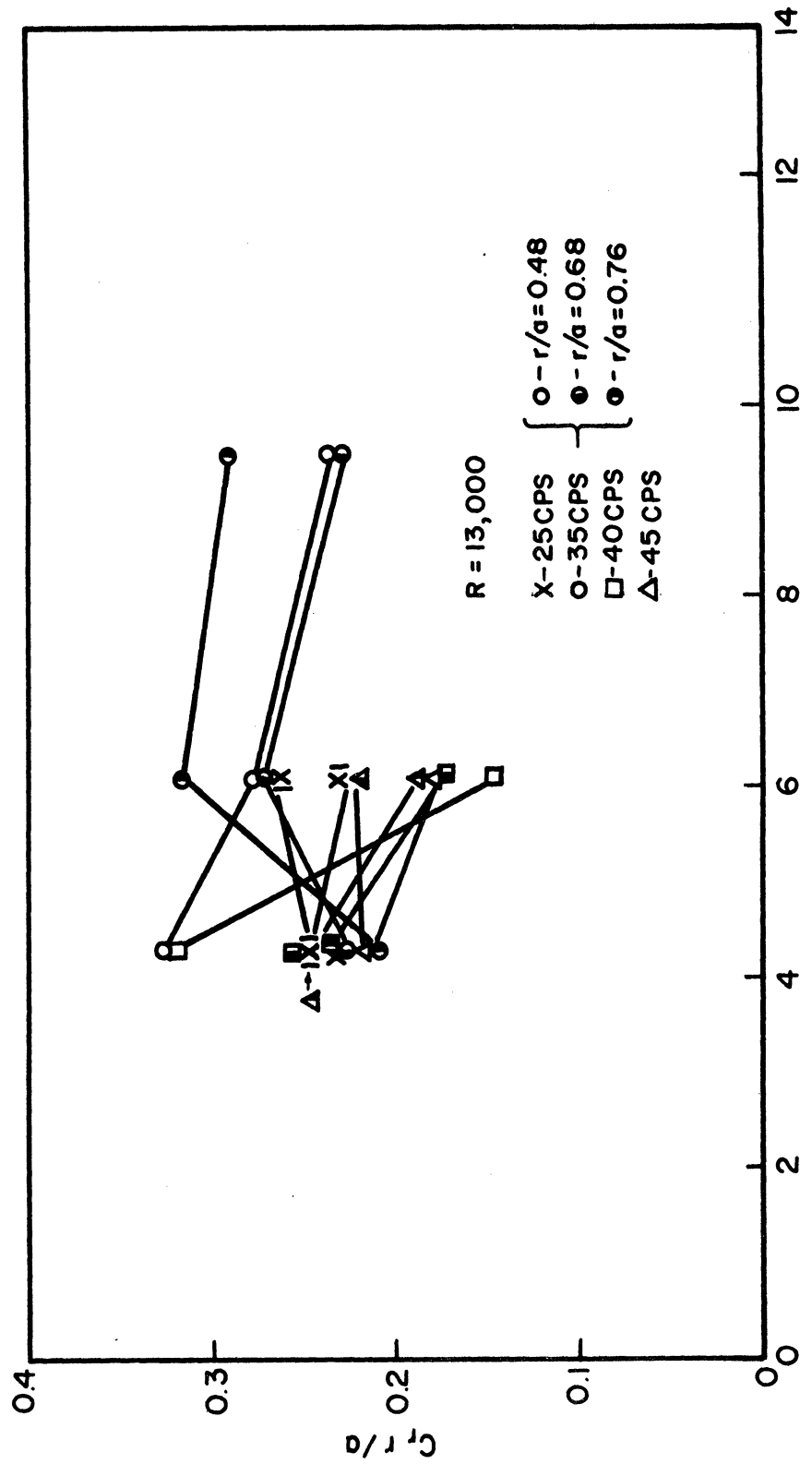

Fig. 41. Longitudinal variation of wave propagation velocity.

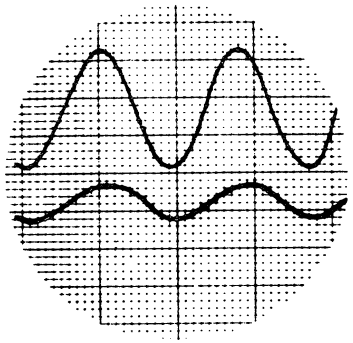

1. Input - 15.5 div.
$u'/u'_{max} = 0.119$

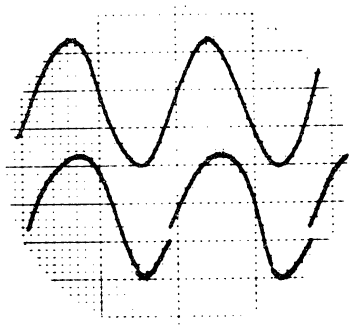

2. Input - 16.5 div.
$u'/u'_{max} = 0.479$

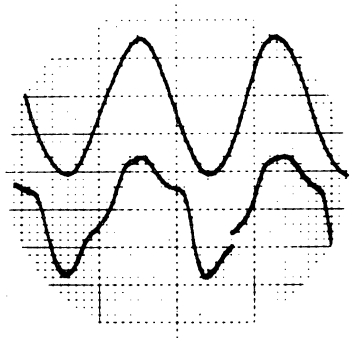

3. Input - 17.5 div.
$u'/u'_{max} = 1.00$

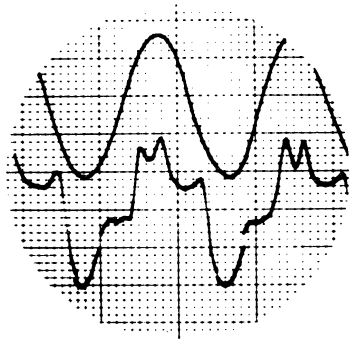

4. Input - 18.5 div.
$u'/u'_{max} = 0.840$

$r/a = 0.568$

R = 4000 f = 25 cps

STATION - 47 dia. downstream of airfoil

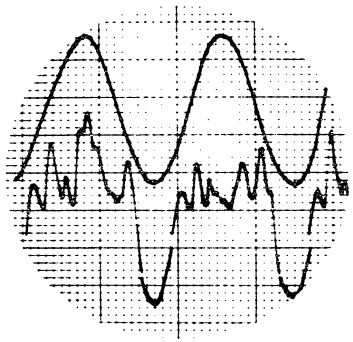

5. Input - 19.0 div.
$u'/u'_{max} = 0.622$

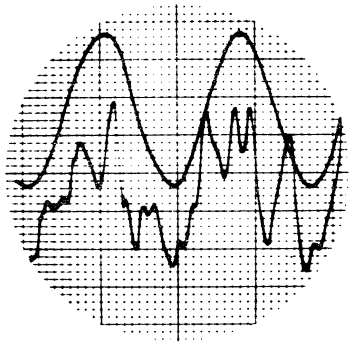

6. Input - 20.0 div.
$u'/u'_{max} = 0.537$

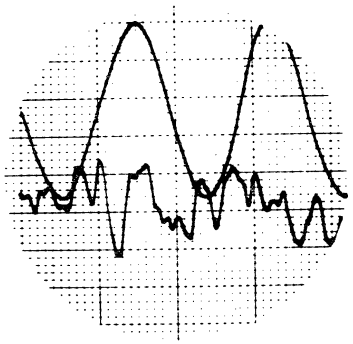

7. Input - 23.0 div.
$u'/u'_{max} = 0.408$

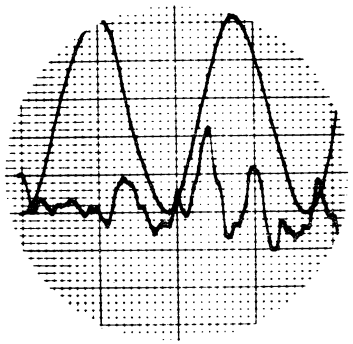

8. Input - 26.0 div.
$u'/u'_{max} = 0.323$

Fig. 42. Distortion of disturbances with increasing amplitude.

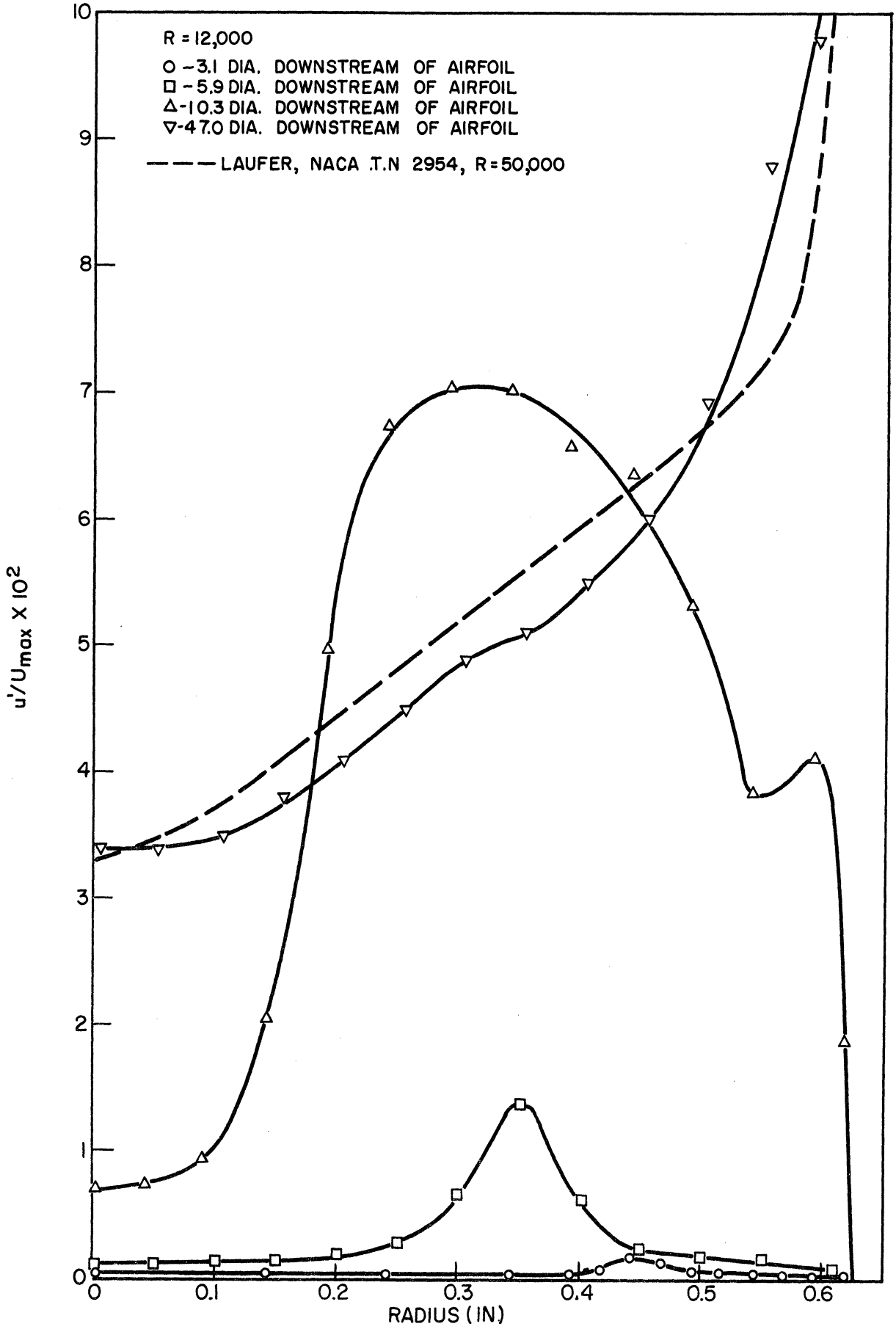

Fig. 43. Radial distribution of turbulent wake of ring airfoil.

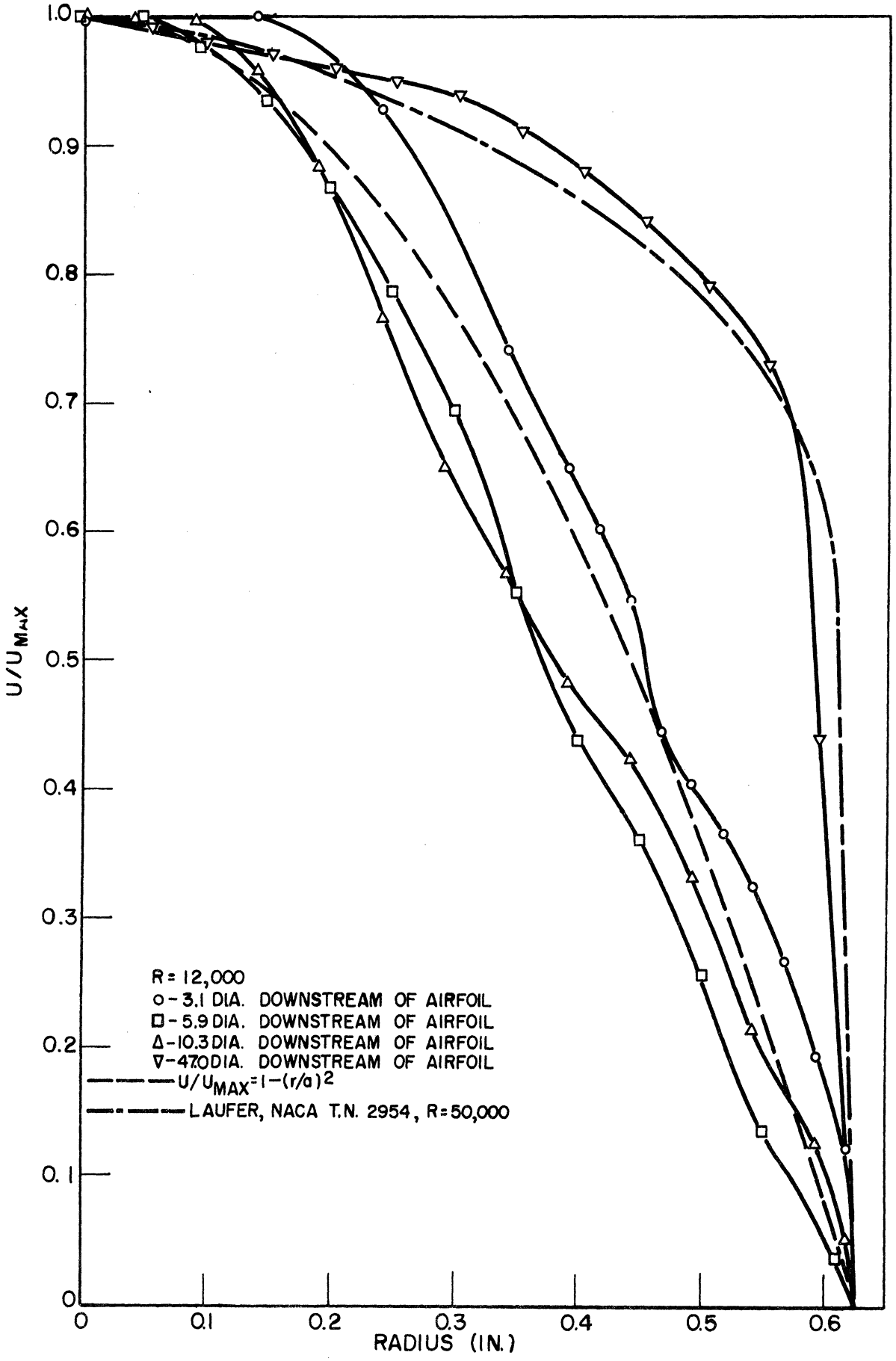

Fig. 44. Mean velocity distributions in region of turbulent wake of ring airfoil.

REFERENCES

1. Orr, W. M. F., Proc. Roy. Irish Acad. 27, 9-26,69-138 (1906-07).

2. Sommerfeld, A., Proc. 4th Int. Congress Appl. Math., Rome, 116-124 (1908).

3. Heisenberg, W., "Über Stabilität und Turbulenz von Flüssigkeitsströmen," Ann. Phys. 74, 577-627 (1924).

4. Tollmien, W., "Ein allgemeines Kriterium der Instabilität laminarer Geschwindigkeitsverteilungen," Nachr. Ges. Wiss., Göttingen, Math.-Phys. Klasse, 79-114 (1935).
   Translation: NACA TM 792 (April 1936).

5. Schlichting, H., "Berechnung der Anfachung kleiner Störungen bei der Plattenströmung," ZAMM 13, 171-174 (1933).

6. Schubauer, G. B., and Skramstad, H. K., Laminar Boundary Layer Oscillations and Stability of Laminar Flow, National Bureau of Standards Research Paper 1772; also J. Aero. Sci. 14, 69-78 (1947); also NACA TR 909 (1948).

7. Lin, C. C., "On the Stability of Two-Dimensional Parallel Flows," Q. Appl. Math. 3, 117-142, 218-234, 277-301 (July and Oct. 1945, and Jan. 1946).

8. Taylor, G. I., "Some Recent Developments in the Study of Turbulence," Proc. 5th Int. Cong. Appl. Mech., 294-310 (1938).

9. Sexl, Th., Ann. Phys. 83, 835-848 (1927); 84, 807-822 (1927).

10. Pekeris, C. L., Phys. Rev. 74, 191 (1948).

11. Sellars, J. R., Some Special Problems in the Stability of Laminar Flows, Ph.D. Thesis, University of Michigan (1952).

12. Corcos, G. M., On the Stability of Poiseuille Flows, Ph.D. Thesis, University of Michigan (1952).

13. Pretsch, J., "Die Stabilität einer Laminarströmung in einem geraden Rohr mit kreisförmigem Querschnitt," ZAMM 21, 204-217 (1941).

14. Corcos, G. M., and Sellars, J. R., On the Stability of Fully Developed Flow in a Pipe, Unpublished (1955).

15. Kovaszany, L. S. G., "Development of Turbulence-Measuring Equipment," NACA TN 2839 (Jan. 1953).

16. Boussinesq, J., Compt. Rend. 113, 9 and 49 (1891).
   See also reference 20, page 22.

17. Squire, H. B., "On the Stability of the Three Dimensional Disturbances of Viscous Fluid Between Parallel Walls," Proc. Roy. Soc., London, (A) 142, 621-629 (1933)

18. Thomas, L. H., "Stability of Plane Poiseuille Flow," Phys. Rev. 91, ser. 2, no. 4, 780-783 (1953).

19. Laufer, John, "The Structure of Turbulence in Fully Developed Pipe Flow," NACA TN 2954 (June 1953).

20. Prandtl, L., and Tietjens, O. G., Applied Hydro and Aeromechanics, McGraw-Hill Book Company, Inc., New York, 1934.

21. Tatsumi, Tomomasa, "Stability of the Laminar Inlet-Flow Prior to the Formation of Poiseuille Regime," J. Phys. Soc. Japan 7, no. 5, 489-502 (1952).

22. Rothfus, R. R., and Prengle, R. S., "Laminar-Turbulent Transition in Smooth Tubes," Ind. and Eng. Chem. 44, no. 7, 1683-1688 (July 1952).

23. Weske, J. R. and Plantholt, A. H., "Discrete Vortex System in the Transition Range of Fully Developed Flow in a Pipe," Readers' Forum, JAS 20, no. 10, 717 (1953).